Can one Hear the Shape of a Drum?

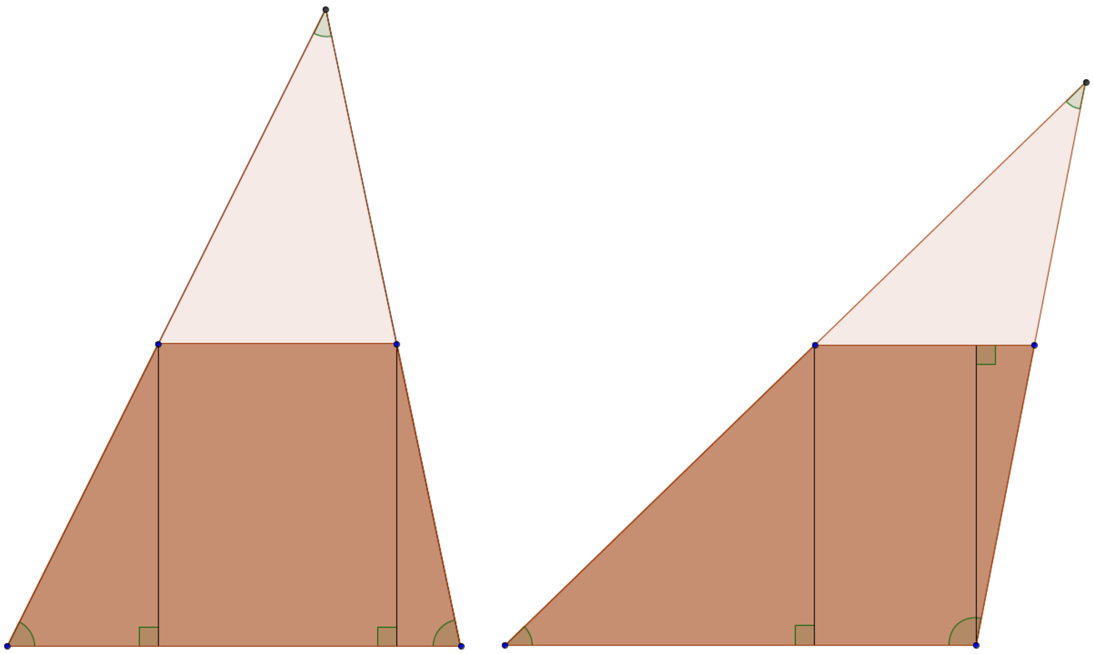

Bachelorthesis Mathematics

Author: Luuk Verhoeven
Supervisor: Dr. Walter van Suijlekom

Cover: Two trapezia that can be determined spectrally (darkly shaded) with their triangle completions (lightly shaded). The triangle completions play an important role in the proof of their spectral determinability, as described in Chapter 4.

Contents

Chapter 1

Introduction

A famous question in mathematics is "Can one hear the shape of a drum?" The question was first phrased this way in 1966 by Mark Kac [10], but the history of this question extends much farther back in time. First, a more concrete statement of the question.

For a bounded domain Ω in $\mathbb{R}^n$ we can define a spectrum as follows. The spectrum of Ω is the multiset of numbers for which

$$\begin{cases} \Delta u(x) + \lambda u(x) = 0 & x \in \Omega, \\ u(x) = 0 & x \in \partial\Omega. \end{cases} \tag{1.1}$$

has a solution. This set of numbers is discrete, positive and has no upper bound [13]. We usually order them into an increasing sequence $\lambda_1 \leq \lambda_2 \leq ... \to \infty$ denoted $(\lambda_n)_{n=1}^{\infty}$.

Computing this spectrum for a given domain Ω is in general very difficult, this is called the (forward) spectral problem. The inverse spectral problem asks one to find geometric properties of Ω, given the spectrum. One of the earliest inverse spectral results is Weyls law, Theorem 1.0.1, which relates the growth of λ_n as a function of n to the area of Ω.

Theorem 1.0.1 (Weyls law). *Defining the eigenvalue counting function*

$$N_+(x) = \#\{n | \lambda_n \leq x\}$$

we have that

$$\lim_{x\to\infty} \frac{N_+(x)}{x^{d/2}} = \frac{\omega_d}{(2\pi)^d} |\Omega| =: c_d, \tag{1.2}$$

where ω_d is the volume of a unit ball in $\mathbb{R}^d$ and $|\Omega|$ is the volume of Ω.

One of the most interesting questions in inverse spectral theory is whether two isospectral domains, i.e. domains with the same spectrum, must be isometric, the appropriate sense of "being the same." This question, specialized to domains in $\mathbb{R}^2$, is what Kac meant with his formulation. The answer of the general question is known to be no, first due to John Milnor in 1964[12]. He provided an example of two isospectral but not isometric 16 dimensional tori. Later, in 1992, Gordon, Webb and Wolpert constructed two isospectral but not isometric domains in $\mathbb{R}^2$ [1], showing that the answer is no also in $\mathbb{R}^2$.

The reason Mark Kac phrased his question as "Can one hear the shape of a drum?" is because in physics the investigation of waves on a domain Ω tells us that the stationary waves that can occur have frequencies corresponding to $c\sqrt{\lambda_n}$ where c is some physical constant related to the speed of waves in the material. So if the answer to Kacs question is positive, one could go to a concert and just listen to the sound the drums make and work out the shape of the drums.

The choice of subject matter for this thesis was inspired by a recent, 2012, result by Grieser and Maronna, they showed that two isospectral triangles must be isometric [5]. In this thesis we will introduce and explore some tools, most importantly traces, for the inverse spectral question, results similar to Weyls theorem, we will also show the proof by Grieser and Maronna for triangular drums and finally attempt to proof some inverse spectral results for quadrilaterals.

Chapter 2

Heat trace

As described in the introduction one of the most important tools for investigating the inverse spectral problem are traces. One of these is the so called heat trace and is the subject of this chapter. The reason the heat trace is useful in providing a link between the spectrum of Δ_Ω and the geometry of Ω is that it can be computed in two different ways, directly from the spectrum and by integrating the heat kernel over Ω.

The heat kernel is an object that arises in the study of the heat equation, which describes how heat moves through idealized solids. The heat equation is

$$\begin{cases} (\partial_t - \Delta_\Omega)u = 0, & \\ u(0,x) = f(x) & x \in \Omega, \\ u(t,x) = 0 & x \in \partial\Omega, \end{cases} \tag{2.1}$$

for some $f(x)$ which represents the initial distribution of heat in the object, $u(t,x)$ is then the temperature at point x and time t.

Solutions can be found using the eigenfunctions of Δ_Ω, since if u_k is the eigenfunction corresponding to eigenvalue $-\lambda_k$ the function $e^{-t\lambda_k}u_k$ satisfies the heat equation[1] and $\{u_k\}_{k=1}^{\infty}$ forms a basis for $L^2(\Omega)$ [13]. Therefore $f = \sum_{k=1}^{\infty} a_k u_k$ where $a_k = \int_\Omega u_k(x)f(x)dx$ and we can write the solution to the heat equation with f as initial condition as

$$u(t,x) = \sum_{k=1}^{\infty} a_k e^{-t\lambda_k} u_k(x), \tag{2.2}$$

$$= \int_\Omega \sum_{k=1}^{\infty} e^{-t\lambda_k} u_k(x) u_k(y) f(y) dy. \tag{2.3}$$

The function $H(t,x,y) := \sum_{k=1}^{\infty} e^{-t\lambda_k} u_k(x) u_k(y)$ is called the heat kernel.

The heat trace $h(t)$ is then given by

$$h(t) = \mathrm{Tr}\left(e^{t\Delta_\Omega}\right), \tag{2.4}$$

$$= \sum_{k=1}^{\infty} e^{-t\lambda_k}, \tag{2.5}$$

$$= \int_\Omega H(t,x,x)dx. \tag{2.6}$$

[1]The minus signs are such that the λ_k are positive.

The second identity shows that the heat trace is a spectral invariant, while the third identity can be used to find certain properties of the heat trace, as exhibited in Section 2.1. In that section we will sketch the proof that Van den Berg and Srisatkunarajah used in [17] to show that the heat trace can be written as

$$h(t) = \frac{A}{4\pi t} - \frac{P}{8\sqrt{\pi t}} + \frac{1}{24}\sum_i \left(\frac{\pi}{\alpha_i} - \frac{\alpha_i}{\pi}\right) + \mathcal{O}\left(e^{-\frac{c}{t}}\right) \tag{2.7}$$

as t tends to zero, for any polygon in $\mathbb{R}^2$ with area A, perimeter P and angles α_i.

These asymptotics will also be verified for certain specific polygons with known spectrum in the section after that. At the end of this chapter we will also give the proof due to Grieser and Maronna that two isospectral triangles must be the same.

2.1 Short Time Asymptotics

In [17], Van den Berg and Srisatkunarajah proof a very useful result about the behaviour of the heat trace $h(t)$ as t tends to zero. We will now sketch the proof of this theorem.

Theorem 2.1.1. *For Ω a polygonal domain in $\mathbb{R}^2$ with vertices of angles α_i, the heat trace as defined in equation 2.4 has the following asymptotic expression as t tends to zero.*

$$h(t) = \frac{A}{4\pi t} - \frac{P}{8\sqrt{\pi t}} + \frac{1}{24}\sum_i \left(\frac{\pi}{\alpha_i} - \frac{\alpha_i}{\pi}\right) + \mathcal{O}\left(e^{-\frac{c}{t}}\right) \tag{2.8}$$

Sketch of proof. The complete proof is somewhat beyond this text and involves many relatively tedious computations, so only a sketch will be provided here. The heat kernel $H(x, y, t)$, or transforms thereof, are known for the plane, the half plane and cones. The central idea is to approximate the heat kernel of Ω by these known variants on pieces of Ω, this idea originates from Kac, who already noted that for t close to zero the spread of heat in an object is only significantly influenced by local properties of the domain. So we approximate the heat kernel near the vertices using the heat kernel for a cone, near the edges we use the heat kernel of the half plane and in the interior we use our knowledge of the heat kernel for the plane to approximate the domains heat kernel. The regions, which are also shown in Figure 2.1 are

$$\begin{aligned} B_i(R) &= \{x \in \Omega | d(x, v_i) < R\} \\ C(\delta, R) &= \{x \in \Omega | d(x, \partial\Omega) < \delta, x \notin \cup_i B_i(R)\} \\ D(\delta, R) &= \{x \in \Omega | x \notin C(\delta, R), x \notin \cup_i B_i(R)\} \end{aligned}$$

where R and δ are parameters that are chosen such that the estimates work out.

For all these different regions we compute a separate estimate between the actual heat kernel H and a approximating heat kernel H'. Van den Berg and Srisatkunarajah compute for $x \in B_i(R)$

$$|H_\Omega(x, x, t) - H_{cone}(x, x, t)| \leq \frac{1}{\pi t} e^{-\frac{R^2}{2t}}, \tag{2.9}$$

for $x \in C(\delta, R)$ they get

$$|H_\Omega(x, x, t) - \frac{1}{4\pi t}(1 - e^{d(x,\partial\Omega)^2/t})| \leq \frac{1}{\pi t} e^{-\frac{R^2 \sin^2(\alpha/2)}{8t}}, \tag{2.10}$$

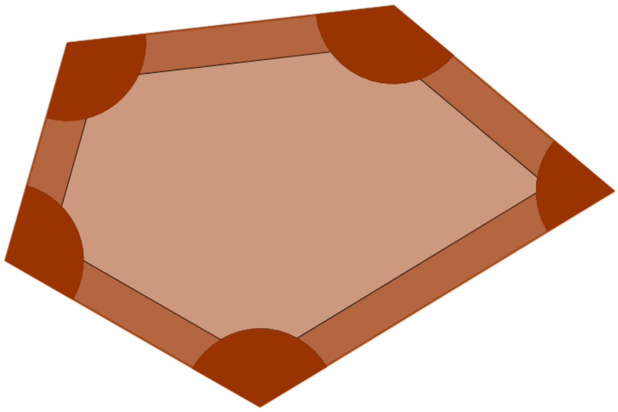

Figure 2.1: This figure shows in what subsections we divide a polygon in order to approximate the heat trace for t near 0. On the dark brown sections the heat kernel is approximated by the heat kernel of a cone, on the lighter brown the heat kernel is approximated by that for a half plane and on the lightest brown area the heat kernel is approximated by that of the complete plane.

and finally for $x \in D(\delta, R)$

$$|H_\Omega(x,x,t) - \frac{1}{4\pi t}| \leq \frac{1}{\pi t} e^{-\frac{R^2 \sin^2(\alpha/2)}{8t}} \tag{2.11}$$

The integral over H_{cone} for a domain of the form $B_i(R)$ has been computed by Van den Berg and Srisatkunarajah, while the other ones are fairly straightforward to integrate over their respective domains. We can now approximate $h(t)$ by writing

$$h(t) = \int_C H_\Omega(x,x,t)dx + \int_D H_\Omega(x,x,t)dx + \sum_i \int_{B_i} H_\Omega(x,x,t)dx \tag{2.12}$$

and using the above estimates for these separate integrals. □

2.2 Explicit Heat Trace Computation

In this section we will verify the asymptotics in Theorem 2.1.1 for three specific types of polygon for which the spectrum is known, facilitating the direct computation of the heat trace. These domains are the rectangle, the isosceles right-angled triangle and the equilateral triangle. The strategy for all three cases will be to relate the heat trace to Jacobi Theta functions and then use a result on the asymptotics of the theta functions, Lemma 2.2.2, to obtain (2.8).

This result for the asymptotics of the Jacobi Theta functions uses the Poisson Summation Formula, a tool from Fourier Analysis.

Theorem 2.2.1 (Poisson Summation Formula). *For $f : \mathbb{R}^n \to \mathbb{R}$, if $f(x) = \int_{\mathbb{R}^n} \hat{f}(\omega) e^{2\pi i x\cdot\omega} d\omega$, where $\hat{f}(\omega) := \int_{\mathbb{R}^n} f(x) e^{-2\pi i \omega\cdot x} dx$ is the Fourier transform of f, and also $|f(x)| \leq A(1+|x|)^{-n-\delta}$ and $|\hat{f}(y)| \leq A(1+|y|)^{-n-\delta}$ for a $\delta > 0$. Then we have*

$$\sum_{m\in\Lambda} f(x+m) = \sum_{m\in\Lambda} \hat{f}(m) e^{2\pi i m\cdot x}, \tag{2.13}$$

and in particular for $x = 0$,

$$\sum_{m\in\Lambda} f(m) = \sum_{m\in\Lambda} \hat{f}(m). \tag{2.14}$$

Here Λ is the lattice of integers $\mathbb{Z}^n$. These series also converge absolutely ([16, Cor. 2.6, p. 252]).

Lemma 2.2.2. *For the Jacobi Theta functions[2] defined by*

$$\begin{aligned} \vartheta_2(q) &:= \sum_{n\in\mathbb{Z}} q^{(n+\frac{1}{2})^2}, & (2.15)\\ \vartheta_3(q) &:= \sum_{n\in\mathbb{Z}} q^{n^2}, & (2.16) \end{aligned}$$

we have that for $q = e^{-a}$ with $a > 0$

$$\begin{aligned} \vartheta_2(q) &= \sqrt{\frac{\pi}{a}} \sum_{n\in\mathbb{Z}} (-1)^n e^{-\frac{\pi^2}{a} n^2} = \sqrt{\frac{\pi}{a}} + \mathcal{O}\left(e^{-\frac{\pi^2/2}{a}}\right), & (2.17)\\ \vartheta_3(q) &= \sqrt{\frac{\pi}{a}} \sum_{n\in\mathbb{Z}} e^{-\frac{\pi^2}{a} n^2} = \sqrt{\frac{\pi}{a}} + \mathcal{O}\left(e^{-\frac{\pi^2/2}{a}}\right), & (2.18) \end{aligned}$$

as a tends to zero.

Proof. We will show this for ϑ_2, the proof for ϑ_3 does not differ in any significant aspect. Define, for $q = e^{-a}$, $f(x) = e^{-a(x+\frac{1}{2})^2}$. This is a scaled and translated Gaussian functions on $\mathbb{R}$ and therefore a Schwartz function, which means that we have that $f(x) = \int_{\mathbb{R}} \hat{f}(\omega) e^{2\pi i x\omega} d\omega$ ([15, Thm. 2.4, p. 182]). The Fourier transform of f is then

$$\hat{f}(\omega) = \sqrt{\frac{\pi}{a}} e^{-\frac{\pi^2}{a}\omega^2} e^{2\pi i \frac{1}{2}\omega}. \tag{2.19}$$

Since this is also a Gaussian function we immediately get the decay conditions on f and $\hat{f}$ required in theorem 2.2.1.

Therefore we can apply the Poisson Sum Formula with dimension 1 to f in order to get

$$\sum_{n\in\mathbb{Z}} e^{-a(n+\frac{1}{2})^2} = \sum_{n\in\mathbb{Z}} \sqrt{\frac{\pi}{a}} e^{-\frac{\pi^2}{a} n^2} e^{\pi i n}, \tag{2.20}$$

which gives us the desired result

$$\vartheta_2(q) = \sqrt{\frac{\pi}{a}} \sum_{n\in\mathbb{Z}} (-1)^n e^{-\frac{\pi^2}{a} n^2}. \tag{2.21}$$

Next we must show our claim about the behaviour as a tends to zero. Since

$$(-1)^n e^{-\frac{\pi^2}{a} n^2} = (-1)^{(-n)} e^{-\frac{\pi^2}{a}(-n)^2} \tag{2.22}$$

[2] As the subscripts suggest, there are more Jacobi Theta functions but they are not required for the following. The Jacobi Theta functions are also normally defined with an extra argument z but this is 0 in all applications of the Jacobi functions in this thesis and therefore also omitted.

we see that (2.21) can be written as

$$\vartheta_2(q) = \sqrt{\frac{\pi}{a}} + 2\sqrt{\frac{\pi}{a}}\sum_{n=1}^{\infty}(-1)^n e^{-\frac{\pi^2}{a}n^2}. \tag{2.23}$$

So to complete the proof for ϑ_2 we must show that

$$\left|2\sqrt{\frac{\pi}{a}}\sum_{n=1}^{\infty}(-1)^n e^{-\frac{\pi^2}{a}n^2}\right| \leq Ce^{-\frac{\pi^2/2}{a}} \tag{2.24}$$

for some $C > 0$ as a tends to zero.

First we will use the geometric series to bound the summation, then we will absorb the $\sqrt{\frac{\pi}{a}}$ factor into the resulting exponential.

$$\begin{aligned}\left|\sum_{n=1}^{\infty}(-1)^n e^{-\frac{\pi^2}{a}n^2}\right| &\leq \sum_{n=1}^{\infty} e^{-\frac{\pi^2}{a}n^2}, \\ &\leq \sum_{n=1}^{\infty} e^{-\frac{\pi^2}{a}n}, \\ &= \frac{e^{-\frac{\pi^2}{a}}}{1-e^{-\frac{\pi^2}{a}}}. \end{aligned} \tag{2.25}$$

When $a < \frac{\pi^2}{\ln(2)}$ we have $e^{-\frac{\pi^2}{a}} < \frac{1}{2}$, so $1 - e^{-\frac{\pi^2}{a}} > \frac{1}{2}$, then for $a < \frac{\pi^2}{\ln(2)}$ we get

$$\left|\sum_{n=1}^{\infty}(-1)^n e^{-\frac{\pi^2}{a}n^2}\right| < 2e^{-\frac{\pi^2}{a}}. \tag{2.26}$$

To eliminate the $\sqrt{\frac{\pi}{a}}$ we use that $\frac{1}{\sqrt{a}} \leq 1 + \frac{1}{a} < e^{\frac{1}{a}} < e^{\frac{\pi^2}{2a}}$. This yields $\sqrt{\frac{\pi}{a}}e^{-\frac{\pi^2}{a}} \leq \sqrt{\pi}e^{\frac{\pi^2}{2a}}e^{-\frac{\pi^2}{a}} = \sqrt{\pi}e^{-\frac{\pi^2}{2a}}$, so to conclude we find that

$$\left|2\sqrt{\frac{\pi}{a}}\sum_{n=1}^{\infty}(-1)^n e^{-\frac{\pi^2}{a}n^2}\right| \leq 2\sqrt{\frac{\pi}{a}} \cdot 2e^{-\frac{\pi^2}{a}} \leq 4\sqrt{\pi}e^{-\frac{\pi^2}{2a}}. \tag{2.27}$$

□

For the rectangle and isosceles right-angled triangle we will often use the following, similar, result.

Lemma 2.2.3. *For $g(x) = \sum_{n\geq 1} e^{-xn^2}$ we have*

$$g(x) = \frac{1}{2}\sqrt{\frac{\pi}{x}} - \frac{1}{2} + \sqrt{\frac{\pi}{x}}g\left(\frac{\pi^2}{x}\right). \tag{2.28}$$

If $x > 0$ we have that

$$g(x) = \frac{1}{2}\sqrt{\frac{\pi}{x}} - \frac{1}{2} + \mathcal{O}\left(e^{-\frac{\pi^2/2}{x}}\right), \tag{2.29}$$

as x tends to zero.

Proof. First of all we see that $2g(x)+1=\vartheta_3(e^{-x})$, so using Lemma 2.2.2 we get

$$2g(x)+1=\sqrt{\frac{\pi}{x}}+\mathcal{O}\left(e^{-\frac{\pi^2/2}{x}}\right), \tag{2.30}$$

which immediately yields (2.29).

To obtain (2.28) we use the first part of (2.17) to get that

$$\begin{aligned}2g(x)+1 &= \sqrt{\frac{\pi}{x}}\sum_{n\in\mathbb{Z}}e^{-\frac{\pi^2}{x}n^2},\\ &= \sqrt{\frac{\pi}{x}}\vartheta_3(e^{-\frac{\pi^2}{x}}),\\ &= \sqrt{\frac{\pi}{x}}(2g\left(\frac{\pi^2}{x}\right)+1).\end{aligned} \tag{2.31}$$

Rewriting this yields

$$g(x)=\frac{1}{2}\sqrt{\frac{\pi}{x}}-\frac{1}{2}+\sqrt{\frac{\pi}{x}}g\left(\frac{\pi^2}{x}\right) \tag{2.32}$$

as desired. □

2.2.1 The Rectangle

The spectrum of a rectangular domain with sides L_x and L_y is

$$\lambda_{m,n}=\pi^2\left(\frac{n^2}{L_x^2}+\frac{m^2}{L_y^2}\right), \tag{2.33}$$

for $m,n\geq 1$. Therefore the heat trace for a rectangular domain becomes

$$h(t)=\sum_{m,n=1}^{\infty}e^{-\pi^2\left(\frac{n^2}{L_x^2}+\frac{m^2}{L_y^2}\right)t}. \tag{2.34}$$

Using the structure of the spectrum of a rectangle combined with the exponential property that $e^{a+b}=e^ae^b$ we see that we can rewrite $h(t)$ to

$$\begin{aligned}h(t) &= \left(\sum_{n=1}^{\infty}e^{-\pi^2\frac{n^2}{L_x^2}t}\right)\left(\sum_{m=1}^{\infty}e^{-\pi^2\frac{m^2}{L_y^2}t}\right),\\ &= g\left(\frac{\pi^2}{L_x^2}t\right)g\left(\frac{\pi^2}{L_y^2}t\right),\end{aligned} \tag{2.35}$$

with $g(x)$ as defined in Lemma 2.2.3. We can now use the relation for g as found in Lemma 2.2.3, Equation 2.29, to find the asymptotics of $h(t)$.

This gives us that

$$\begin{aligned}h(t) &= \left(\frac{1}{2}\sqrt{\frac{\pi}{\frac{\pi^2}{L_x^2}t}}-\frac{1}{2}+\mathcal{O}\left(e^{-\frac{\pi^2/2}{\pi^2/L_x^2t}}\right)\right)\left(\frac{1}{2}\sqrt{\frac{\pi}{\frac{\pi^2}{L_y^2}t}}-\frac{1}{2}+\mathcal{O}\left(e^{-\frac{\pi^2/2}{\pi^2/L_y^2t}}\right)\right),\\ &= \left(\frac{1}{2}\frac{L_x}{\sqrt{\pi t}}-\frac{1}{2}+\mathcal{O}\left(e^{-\frac{L_x^2}{2t}}\right)\right)\left(\frac{1}{2}\frac{L_y}{\sqrt{\pi t}}-\frac{1}{2}+\mathcal{O}\left(e^{-\frac{L_y^2}{2t}}\right)\right).\end{aligned} \tag{2.36}$$

In order to proceed from here we will use some useful properties of the $\mathcal{O}\left(e^{-\frac{c}{t}}\right)$.

Lemma 2.2.4. *If $f(t)$ is $\mathcal{O}\left(e^{-\frac{c_1}{t}}\right)$ and $g(t)$ is $\mathcal{O}\left(e^{-\frac{c_2}{t}}\right)$ for $c_1, c_2 > 0$ as t tends to zero, we have*

1. *fg is $\mathcal{O}\left(e^{-\frac{c_1+c_2}{t}}\right)$,*

2. *$f+g$ is $\mathcal{O}\left(e^{-\frac{\min(c_1,c_2)}{t}}\right)$,*

3. *$\frac{1}{t}f$ is $\mathcal{O}\left(e^{-\frac{c_1}{2t}}\right)$.*

4. *$\frac{1}{\sqrt{t}}f$ is $\mathcal{O}\left(e^{-\frac{c_1}{2t}}\right)$,*

Proof. **Property 1:** Suppose $|f(t)| \leq C_1 e^{-\frac{c_1}{t}}$ for $t < t_1$ and $|g(t)| \leq C_2 e^{-\frac{c_2}{t}}$ for $t < t_2$. Then $|fg| = |f||g| \leq C_1 C_2 e^{-\frac{c_1}{t}} e^{-\frac{c_2}{t}} = C_1 C_2 e^{-\frac{c_1+c_2}{t}}$ for $t < \min(t_1, t_2)$. Therefore fg is $\mathcal{O}\left(e^{-\frac{c_1+c_2}{t}}\right)$.
Property 2: Reusing the definitions from the previous property we get $|f+g| \leq |f|+|g| \leq C_1 e^{-\frac{c_1}{t}} + C_2 e^{-\frac{c_2}{t}}$ for $t < \min(t_1, t_2)$. Since $e^{-\frac{c_i}{t}} \leq e^{-\frac{\min(c_1,c_2)}{t}}$ for $i = 1, 2$ we then get $|f+g| \leq (C_1 + C_2) e^{-\frac{\min(c_1,c_2)}{t}}$ for $t < \min(t_1, t_2)$, so $f+g$ is $\mathcal{O}\left(e^{-\frac{\min(c_1,c_2)}{t}}\right)$.
Property 3: Again reusing the above definitions we have that $|\frac{1}{t}f(t)| \leq \frac{1}{t}C_1 e^{-\frac{c_1}{t}} = C_1\left(\frac{1}{t}e^{-\frac{c_1}{2t}}\right)e^{-\frac{c_1}{2t}}$. So if we can show that $\frac{1}{t}e^{-\frac{c_1}{2t}}$ is bounded, say by B, for t near zero it follows that $|\frac{1}{t}f(t)| \leq C_1 B e^{-\frac{c_1}{2t}}$. To show this we will compute

$$\lim_{t\to 0} \frac{1}{t} e^{-\frac{c}{2t}} \tag{2.37}$$

using L'Hôpital's rule, as follows.

$$\begin{aligned}
\lim_{t\to 0} \frac{1}{t} e^{-\frac{c}{2t}} &= \lim_{t\to 0} \frac{\frac{1}{t}}{e^{\frac{c}{2t}}}, \\
&= \lim_{t\to 0} \frac{-\frac{1}{t^2}}{-\frac{c}{2t^2} e^{\frac{c}{2t}}}, \\
&= \lim_{t\to 0} \frac{2}{c e^{\frac{c}{2t}}}, \\
&= 0.
\end{aligned} \tag{2.38}$$

Since $\frac{1}{t}e^{-\frac{c}{2t}} \leq \frac{1}{t}$ we also get that $\lim_{t\to\infty} \frac{1}{t}e^{-\frac{c}{2t}} = 0$. Therefore continuity of $\frac{1}{t}e^{-\frac{c}{2t}}$ for $t > 0$ implies that $\frac{1}{t}e^{-\frac{c}{2t}}$ is bounded by some B for all t, so certainly near zero.
Property 4: Since for $t < 1$ we have that $\frac{1}{t} > \frac{1}{\sqrt{t}}$ this is implied by property 3. □

Using this lemma we can expand the brackets in (2.36), and make sense of the order terms, where we also assume $L_x < L_y$ without loss of generality.

$$\begin{aligned}
h(t) &= \left(\frac{1}{2}\frac{L_x}{\sqrt{\pi t}} - \frac{1}{2} + \mathcal{O}\left(e^{-\frac{L_x^2}{2t}}\right)\right)\left(\frac{1}{2}\frac{L_y}{\sqrt{\pi t}} - \frac{1}{2} + \mathcal{O}\left(e^{-\frac{L_y^2}{2t}}\right)\right), \\
&= \frac{A}{4\pi t} - \frac{1}{4}\frac{L_x + L_y}{\sqrt{\pi t}} + \frac{1}{4} + \frac{1}{2}\frac{L_x}{\sqrt{\pi t}}\mathcal{O}\left(e^{-\frac{L_y^2}{2t}}\right) - \frac{1}{2}\mathcal{O}\left(e^{-\frac{L_y^2}{2t}}\right) \\
&\quad + \frac{1}{2}\frac{L_y}{\sqrt{\pi t}}\mathcal{O}\left(e^{-\frac{L_x^2}{2t}}\right) - \frac{1}{2}\mathcal{O}\left(e^{-\frac{L_x^2}{2t}}\right) + \mathcal{O}\left(e^{-\frac{L_x^2}{2t}}\right)\mathcal{O}\left(e^{-\frac{L_y^2}{2t}}\right), \quad (2.39) \\
&= \frac{A}{4\pi t} - \frac{P}{8\sqrt{\pi t}} + \frac{1}{4} + \mathcal{O}\left(e^{-\frac{L_y^2}{4t}}\right) + \mathcal{O}\left(e^{-\frac{L_y^2}{2t}}\right) \\
&\quad + \mathcal{O}\left(e^{-\frac{L_x^2}{4t}}\right) + \mathcal{O}\left(e^{-\frac{L_x^2}{2t}}\right) + \mathcal{O}\left(e^{-\frac{L_x^2+L_y^2}{2t}}\right), \quad (2.40) \\
&= \frac{A}{4\pi t} - \frac{P}{8\sqrt{\pi t}} + \frac{1}{4} + \mathcal{O}\left(e^{-\frac{L_y^2}{4t}}\right) + \mathcal{O}\left(e^{-\frac{L_x^2}{4t}}\right) + \mathcal{O}\left(e^{-\frac{L_x^2}{t}}\right), \quad (2.41) \\
&= \frac{A}{4\pi t} - \frac{P}{8\sqrt{\pi t}} + \frac{1}{4} + \mathcal{O}\left(e^{-\frac{L_x^2}{4t}}\right), \quad (2.42)
\end{aligned}$$

were we used $A = L_x L_y$ and $P = 2(L_x + L_y)$. Since for the rectangle we have four vertices with $\alpha_i = \frac{\pi}{2}$, this corresponds to the content of Theorem 2.1.1, proving the general theorem for the specific case of rectangular domains.

As a bonus, Equation 2.28 from Lemma 2.2.3 allows us to compute an explicit, though not elementary, expression for the heat trace of a rectangle.

$$\begin{aligned}
h(t) &= g\left(\frac{\pi^2}{L_x^2}t\right) g\left(\frac{\pi^2}{L_y^2}t\right), \\
&= \left(\frac{1}{2}\sqrt{\frac{\pi}{\frac{\pi^2}{L_x^2}t}} - \frac{1}{2} + \sqrt{\frac{\pi}{\frac{\pi^2}{L_x^2}t}}\, g\left(\frac{\pi^2}{\frac{\pi^2}{L_x^2}t}\right)\right)\left(\frac{1}{2}\sqrt{\frac{\pi}{\frac{\pi^2}{L_y^2}t}} - \frac{1}{2} + \sqrt{\frac{\pi}{\frac{\pi^2}{L_y^2}t}}\, g\left(\frac{\pi^2}{\frac{\pi^2}{L_y^2}t}\right)\right), \\
&= \left(\frac{1}{2}\frac{L_x}{\sqrt{\pi t}} - \frac{1}{2} + \frac{L_x}{\sqrt{\pi t}} g\left(\frac{L_x^2}{t}\right)\right)\left(\frac{1}{2}\frac{L_y}{\sqrt{\pi t}} - \frac{1}{2} + \frac{L_y}{\sqrt{\pi t}} g\left(\frac{L_y^2}{t}\right)\right), \\
&= \frac{L_x L_y}{4\pi t} - \frac{L_x + L_y}{4\sqrt{\pi t}} + \frac{1}{4} + \left(\frac{1}{2}\frac{L_y}{\sqrt{\pi t}} - \frac{1}{2}\right)\frac{L_x}{\sqrt{\pi t}} g\left(\frac{L_x^2}{t}\right) + \\
&\quad \left(\frac{1}{2}\frac{L_x}{\sqrt{\pi t}} - \frac{1}{2}\right)\frac{L_y}{\sqrt{\pi t}} g\left(\frac{L_y^2}{t}\right) + \frac{L_x}{\sqrt{\pi t}} g\left(\frac{L_x^2}{t}\right)\frac{L_y}{\sqrt{\pi t}} g\left(\frac{L_y^2}{t}\right). \quad (2.43)
\end{aligned}$$

Since we have that $A = L_x L_y$, $P = 2(L_x + L_y)$ we get that

$$\begin{aligned}
h(t) &= \frac{A}{4\pi t} - \frac{P}{8\sqrt{\pi t}} + \frac{1}{4} + \left(\frac{A}{2\pi t} - \frac{L_y}{2\sqrt{\pi t}}\right)\sum_{n=1}^{\infty} e^{-\frac{L_x^2}{t}n^2} \\
&\quad + \left(\frac{A}{2\pi t} - \frac{L_x}{2\sqrt{\pi t}}\right)\sum_{m=1}^{\infty} e^{-\frac{L_y^2}{t}m^2} + \frac{A}{\pi t}\sum_{m,n=1}^{\infty} e^{-\left(\frac{L_x^2}{t}n^2 + \frac{L_y^2}{t}m^2\right)}, \quad (2.44)
\end{aligned}$$

where we also replaced $g(x)$ by its definition. This expression is interesting in combination with some information from Chapter 3 on the wave trace. The exponents all carry factors that are squares of lengths of periodic orbits, which is interesting in combination with the Poisson relation from Section 3.2.1, maybe suggesting a deeper link between the wave and heat traces, although this might also be a fluke.

2.2.2 The Isosceles Right-angled Triangle

The spectrum of a isosceles right-angled triangle with cathetis of length a is [4]

$$\lambda_{m,n} = \frac{\pi^2}{a^2}((m+n)^2 + n^2), \tag{2.45}$$

for $m, n \geq 1$. Then we get

$$h(t) = \sum_{m,n=1}^{\infty} e^{-\frac{\pi^2}{a^2}((m+n)^2+n^2)t}. \tag{2.46}$$

In this case we will rewrite the sums, which are positive and convergent, therefore absolutely convergent, to get the heat trace to a form where we can apply Lemma 2.2.3. For notational purposes we define

$$f(x,y) = e^{-\frac{\pi^2}{a^2}(x^2+y^2)t} \tag{2.47}$$

such that

$$h(t) = \sum_{m,n=1}^{\infty} f(m+n,n) = \sum_{n=1}^{\infty}\sum_{m=n+1}^{\infty} f(m,n). \tag{2.48}$$

Since $f(m,n) = f(n,m)$ we get that

$$\begin{aligned}
\sum_{n=1}^{\infty}\sum_{m=n+1}^{\infty} f(m,n) &= \sum_{n=1}^{\infty}\sum_{m=n+1}^{\infty} f(n,m), \\
&= \sum_{m=1}^{\infty}\sum_{n=m+1}^{\infty} f(m,n), \qquad (2.49) \\
&= \sum_{n=1}^{\infty}\sum_{m=1}^{n-1} f(m,n). \qquad (2.50)
\end{aligned}$$

Therefore we find that

$$\begin{aligned}
\sum_{n=1}^{\infty}\sum_{m=1}^{\infty} f(m,n) &= \sum_{n=1}^{\infty}\sum_{m=1}^{n-1} f(m,n) + \sum_{n=1}^{\infty}\sum_{m=n+1}^{\infty} f(m,n) + \sum_{n=1}^{\infty} f(n,n), \\
&= 2h(t) + \sum_{n=1}^{\infty} f(n,n). \qquad (2.51)
\end{aligned}$$

Or more explicitly

$$\sum_{n=1}^{\infty}\sum_{m=1}^{\infty} e^{-\frac{\pi^2}{a^2}(m^2+n^2)t} = 2h(t) + \sum_{n=1}^{\infty} e^{-\frac{\pi^2}{a^2}(n^2+n^2)t}. \tag{2.52}$$

The left hand side of (2.52) is the heat trace of a rectangle with both sides length a, and the sum in the right hand side is $g\left(\frac{2\pi^2}{a^2}t\right)$. Reorganizing the terms in (2.52) and applying the known expressions for the heat trace of a rectangle and the function g we find that

$$\begin{aligned} h(t) &= \frac{1}{2}\left(\frac{a^2}{4\pi t} - \frac{4a}{8\sqrt{\pi t}} + \frac{1}{4} + \mathcal{O}\left(e^{-\frac{a^2}{4t}}\right)\right) - \frac{1}{2}\left(\frac{1}{2}\sqrt{\frac{\pi}{\frac{2\pi^2}{a^2}t}} - \frac{1}{2} + \mathcal{O}\left(e^{-\frac{\pi^2/2}{\frac{2\pi^2}{a^2}t}}\right)\right) \\ &= \frac{\frac{1}{2}a^2}{4\pi t} - \frac{2a}{8\sqrt{\pi t}} + \frac{1}{8} + \mathcal{O}\left(e^{-\frac{a^2}{4t}}\right) - \frac{a}{4\sqrt{2\pi t}} + \frac{1}{4} + \mathcal{O}\left(e^{-\frac{a^2}{4t}}\right) \qquad (2.53) \\ &= \frac{\frac{1}{2}a^2}{4\pi t} - \frac{2a + \sqrt{2}a}{8\sqrt{\pi t}} + \frac{3}{8} + \mathcal{O}\left(e^{-\frac{a^2}{4t}}\right), \qquad (2.54) \end{aligned}$$

which corresponds exactly to (2.8) and thus proofs Theorem 2.1.1 for the isosceles right-angled triangle with catheti of length a. This same computation is performed in [4].

2.2.3 The Equilateral Triangle

The spectrum of a equilateral triangle with radius of the inscribed circle r is [11]

$$\lambda_{m,n} = \frac{4}{27}\frac{\pi^2}{r^2}(m^2 + mn + n^2), \qquad (2.55)$$

again for $m, n \geq 1$.

For brevity we will define

$$q = e^{-\frac{4}{27}\frac{\pi^2}{r^2}t}, \qquad (2.56)$$

so that

$$h(t) = \sum_{m,n=1}^{\infty} q^{m^2+mn+n^2}. \qquad (2.57)$$

In the computation of this heat trace we will use an auxiliary function

$$\bar{h}(t) = \sum_{m,n=1}^{\infty} q^{m^2-mn+n^2} = \sum_{m=1}^{\infty}\sum_{n=-1}^{-\infty} q^{m^2+mn+n^2}. \qquad (2.58)$$

First we will compute $h(t) + \bar{h}(t)$, which turns out to be expressible using only Jacobi Theta functions, then we will compute $\bar{h}(t) - h(t)$, which turns out to be relatable to $\bar{h}(t)$ in such a way that we can solve the resulting set of equations for $h(t)$.

An important tool in these computations will be the following lemma

Lemma 2.2.5. *For*

$$\begin{aligned} \phi &: \mathbb{Z}^2 \to \mathbb{Z}^2 \\ (x, y) &\mapsto (2x + y, y) \end{aligned}$$

we have

$$\sum_{(x,y)\in D} q^{x^2+xy+y^2} = \sum_{(n,m)\in\phi(D)} q^{\frac{n^2+3m^2}{4}}, \qquad (2.59)$$

for $0 < q < 1$ *and* $D \subset \mathbb{Z}^2$.

Proof. To show this we need that ϕ is injective on $\mathbb{Z}^2$ and therefore bijective between D and $\phi(D)$, and that for $(n,m) = \phi(x,y)$ we have that $x^2 + xy + y^2 = \frac{1}{4}(n^2 + 3m^2)$. First, suppose $(n,m) = \phi(x_1,y_1) = \phi(x_2,y_2)$. Then immediately $y_1 = m = y_2$, so $2x_1 + y_1 = 2x_1 + y_2 = n = 2x_2 + y_2$, therefore $x_1 = x_2$ and we conclude that ϕ is injective. For the second part we see that

$$\begin{aligned}\frac{1}{4}(n^2 + 3m^2) &= \frac{1}{4}((2x+y)^2 + 3y^2),\\ &= \frac{1}{4}(4x^2 + 4xy + y^2 + 3y^2),\\ &= x^2 + xy + y^2.\end{aligned}$$

□

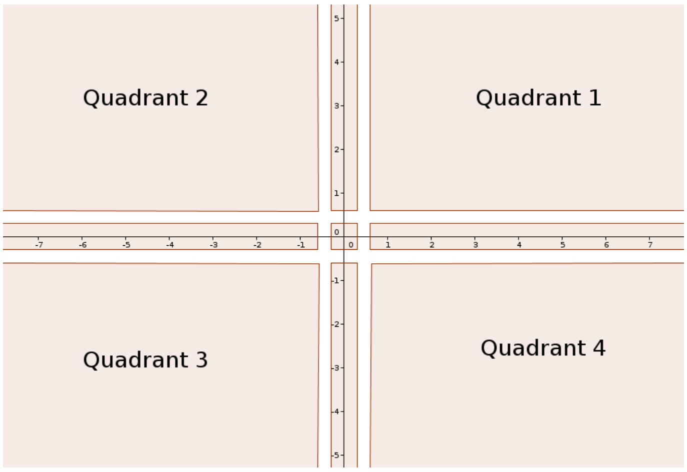

Figure 2.2: An image of the subdivision of $\mathbb{Z}^2$ into quadrants, axes and the center.

Now for the computation of $h(t) + \bar{h}(t)$. First we notice that we can divide $\mathbb{Z}^2$ into the disjoint union of the four quadrants $\{(x,y)| \pm x \geq 1, \pm y \geq 1\}$, the four axial directions $\{(x,0)| \pm x \geq 1\}$ and $\{(0,x)| \pm x \geq 1\}$ and the center $\{(0,0)\}$. Then, if we compute the sum of $q^{x^2+xy+y^2}$ over $\mathbb{Z}^2$, we can separate the sum into these 9 parts and recognize that quadrant 1 and 3, see Figure 2.2, both correspond to $h(t)$ whereas quadrants 2 and 4 correspond to $\bar{h}(t)$, for the appropriate choice of q. Furthermore, the sums over all 4 axis terms are the same, since they all have either x or y zero. This leads us to

$$\sum_{(x,y)\in\mathbb{Z}^2} q^{x^2+xy+y^2} = 2h(t) + 2\bar{h}(t) + 4\sum_{x=1}^{\infty} q^{x^2} + 1, \tag{2.60}$$

or when transformed to use Jacobi Theta functions

$$\sum_{(x,y)\in\mathbb{Z}^2} q^{x^2+xy+y^2} = 2h(t) + 2\bar{h}(t) + 2\vartheta_3(q) - 1. \tag{2.61}$$

In order to evaluate the left hand side of (2.61) we use Lemma 2.2.5 with $D = \mathbb{Z}^2$. Then $\phi(D) = \{(n,m) \in \mathbb{Z}^2 | n, m \text{ same parity}\}$, so we get

$$\sum_{(x,y)\in\mathbb{Z}^2} q^{x^2+xy+y^2} = \sum_{\substack{(n,m)\in\mathbb{Z}^2\\ n,m \text{ both even}}} q^{\frac{n^2+3m^2}{4}} + \sum_{\substack{(n,m)\in\mathbb{Z}^2\\ n,m \text{ both odd}}} q^{\frac{n^2+3m^2}{4}}. \tag{2.62}$$

We can rewrite this equation to

$$\begin{aligned}
\sum_{(x,y)\in\mathbb{Z}^2} q^{x^2+xy+y^2} &= \sum_{(n,m)\in\mathbb{Z}^2} q^{\frac{(2n)^2+3(2m)^2}{4}} + \sum_{(n,m)\in\mathbb{Z}^2} q^{\frac{(2n+1)^2+3(2m+1)^2}{4}}, \\
&= \sum_{n\in\mathbb{Z}} q^{\frac{1}{4}(2n)^2} \sum_{m\in\mathbb{Z}} q^{\frac{3}{4}(2m)^2} + \sum_{n\in\mathbb{Z}} q^{\frac{1}{4}(2n+1)^2} \sum_{m\in\mathbb{Z}} q^{\frac{3}{4}(2m+1)^2}, \\
&= \sum_{n\in\mathbb{Z}} q^{n^2} \sum_{m\in\mathbb{Z}} (q^3)^{m^2} + \sum_{n\in\mathbb{Z}} q^{(n+\frac{1}{2})^2} \sum_{m\in\mathbb{Z}} (q^3)^{(m+\frac{1}{2})^2}, \\
&= \vartheta_3(q)\vartheta_3(q^3) + \vartheta_2(q)\vartheta_2(q^3). \qquad (2.63)
\end{aligned}$$

This allows us to find our final expression for $h(t) + \bar{h}(t)$

$$h(t) + \bar{h}(t) = \frac{1}{2}\left(\vartheta_3(q)\vartheta_3(q^3) + \vartheta_2(q)\vartheta_2(q^3)\right) - \vartheta_3(q) + \frac{1}{2}. \qquad (2.64)$$

The next step in our calculation is to find an expression for $\bar{h}(t) - h(t)$. To do this we recognize that $\bar{h}(t)$ and $h(t)$ are both sums of $q^{x^2+xy+y^2}$ on different domains, allowing us to apply Lemma 2.2.5 to both. For $h(t)$ this domain $D = \{(x, y) \in \mathbb{Z}^2 | x \geq 1, y \geq 1\}$ and for $\bar{h}(t)$ the domain is $D' = \{(x, y) \in \mathbb{Z}^2 | x \leq -1, y \geq 1\}$. Then $\phi(D) = \{(n, m) \in \mathbb{Z}^2 | m > 0; n > m; n, m \text{ same parity}\}$ and $\phi(D') = \{(n, m) \in \mathbb{Z}^2 | m > 0; n < m; n, m \text{ same parity}\}$. Since we are interested in the difference of $\bar{h}(t)$ and $h(t)$ we transform $\phi(D)$ again by taking $-n$ instead of n. Because the summand depends only on n^2 this doesn't change $\sum_{(n,m)\in\phi(D)} q^{\frac{1}{4}(n^2+3m^2)}$ and we get

$$\begin{aligned}
\bar{h}(t) - h(t) &= \sum_{(n,m)\in\phi(D')} q^{\frac{1}{4}(n^2+3m^2)} - \sum_{(n,m)\in\phi(D)} q^{\frac{1}{4}(n^2+3m^2)}, \\
&= \sum_{(n,m)\in\phi(D')} q^{\frac{1}{4}(n^2+3m^2)} - \sum_{(-n,m)\in\phi(D)} q^{\frac{1}{4}((-n)^2+3m^2)}, \\
&= \sum_{\substack{(n,m)\in\phi(D') \\ (-n,m)\notin\phi(D)}} q^{\frac{1}{4}(n^2+3m^2)}. \qquad (2.65)
\end{aligned}$$

In order to proceed we simplify the domain of summation in (2.65), the domain is

$$\begin{aligned}
&\{(n, m) \in \mathbb{Z}^2 | (n, m) \in \phi(D'), (-n, m) \notin \phi(D)\} \\
&\quad = \{(n, m) \in \mathbb{Z}^2 | m > 0; n < m; n, m \text{ same parity}; \neg(-n > m)\}, \\
&\quad = \{(n, m) \in \mathbb{Z}^2 | m > 0; -m \leq n < m; n, m \text{ same parity}\}, \\
&\quad = \{(n, m) \in \mathbb{Z}^2 | m > 0; -m < n < m; n, m \text{ same parity}\} \cup \{(-n, n) | n \in \mathbb{Z}_{>0}\}. \qquad (2.66)
\end{aligned}$$

The first part of this domain turns out to be the transformation, $\phi(D'')$, of $D'' = \{(x, y) \in \mathbb{Z}^2 | y > 0, -y < x < 0\}$. These considerations together yield

$$\begin{aligned}
\bar{h}(t) - h(t) &= \sum_{(n,m)\in\phi(D'')} q^{\frac{n^2+3m^2}{4}} + \sum_{n\in\mathbb{Z}_{>0}} q^{\frac{(-n)^2+3n^2}{4}}, \\
&= \sum_{(x,y)\in D''} q^{x^2+xy+y^2} + \sum_{n\in\mathbb{Z}_{>0}} q^{n^2}, \\
&= \sum_{\substack{(x,y)\in\mathbb{Z}^2 \\ y>0,-y<x<0}} q^{x^2+xy+y^2} + \sum_{n\in\mathbb{Z}_{>0}} q^{n^2}. \qquad (2.67)
\end{aligned}$$

Changing x to $-x$ in the sum then yields

$$\bar{h}(t) - h(t) = \sum_{\substack{(x,y)\in\mathbb{Z}^2 \\ y>0, 0<x<y}} q^{x^2-xy+y^2} + \sum_{n\in\mathbb{Z}_{>0}} q^{n^2}. \tag{2.68}$$

The sum in (2.68) can be easily related to $\bar{h}(t)$ by noticing that the summand in $\bar{h}(t)$ is invariant under exchange of x and y, such that

$$\begin{aligned} \bar{h}(t) &= \sum_{\substack{(x,y)\in\mathbb{Z}^2 \\ y>0, 0<x<y}} q^{x^2-xy+y^2} + \sum_{\substack{(x,y)\in\mathbb{Z}^2 \\ x>0, 0<y<x}} q^{x^2-xy+y^2} + \sum_{(x,x), x\in\mathbb{Z}_{>0}} q^{x^2}, \\ &= 2\sum_{\substack{(x,y)\in\mathbb{Z}^2 \\ y>0, 0<x<y}} q^{x^2-xy+y^2} + \sum_{(x,x), x\in\mathbb{Z}_{>0}} q^{x^2}. \end{aligned} \tag{2.69}$$

Using this equality we find that (2.68) becomes

$$\bar{h}(t) - h(t) = \frac{1}{2}\left(\bar{h}(t) - \sum_{x\in\mathbb{Z}_{>0}} q^{x^2}\right) + \sum_{n\in\mathbb{Z}_{>0}} q^{n^2}, \tag{2.70}$$

which we can rewrite to

$$\bar{h}(t) - 2h(t) = \sum_{n\in\mathbb{Z}_{>0}} q^{n^2} = \frac{1}{2}(\vartheta_3(q) - 1). \tag{2.71}$$

Now that we have explicit expressions for $\bar{h}(t) + h(t)$ and $\bar{h}(t) - 2h(t)$ in terms of Jacobi Theta functions we can solve for $h(t)$.

$$\begin{aligned} h(t) &= \frac{1}{3}([h(t) + \bar{h}(t)] - [\bar{h}(t) - 2h(t)]), \\ &= \frac{1}{3}(\frac{1}{2}\left(\vartheta_3(q)\vartheta_3(q^3) + \vartheta_2(q)\vartheta_2(q^3)\right) - \vartheta_3(q) + \frac{1}{2} - \frac{1}{2}(\vartheta_3(q) - 1)), \\ &= \frac{1}{6}\left(\vartheta_3(q)\vartheta_3(q^3) + \vartheta_2(q)\vartheta_2(q^3)\right) - \frac{1}{2}\vartheta_3(q) + \frac{1}{3}. \end{aligned} \tag{2.72}$$

This allows us to apply Lemma 2.2.2, as well as our properties from Lemma 2.2.4. We find that, for $q = e^{-a} = e^{-\frac{4}{27}\frac{\pi^2}{r^2}t}$,

$$\begin{aligned} h(t) &= \frac{1}{6}\left(\sqrt{\frac{\pi}{a}} + \mathcal{O}\left(e^{-\frac{\pi^2/2}{a}}\right)\right)\left(\sqrt{\frac{\pi}{3a}} + \mathcal{O}\left(e^{-\frac{\pi^2/2}{3a}}\right)\right) \\ &\quad + \frac{1}{6}\left(\sqrt{\frac{\pi}{a}} + \mathcal{O}\left(e^{-\frac{\pi^2/2}{a}}\right)\right)\left(\sqrt{\frac{\pi}{3a}} + \mathcal{O}\left(e^{-\frac{\pi^2/2}{3a}}\right)\right) - \frac{1}{2}\sqrt{\frac{\pi}{a}} + \mathcal{O}\left(e^{-\frac{\pi^2/2}{a}}\right) + \frac{1}{3}, \\ &= \frac{1}{6}\left(\frac{\pi}{\sqrt{3}a} + \mathcal{O}\left(e^{-\frac{\pi^2}{12a}}\right) + \frac{\pi}{\sqrt{3}a} + \mathcal{O}\left(e^{-\frac{\pi^2}{12a}}\right)\right) - \frac{1}{2}\sqrt{\frac{\pi}{a}} + \mathcal{O}\left(e^{-\frac{\pi^2/2}{a}}\right) + \frac{1}{3}, \\ &= \frac{\pi}{3\sqrt{3}a} - \frac{1}{2}\sqrt{\frac{\pi}{a}} + \frac{1}{3} + \mathcal{O}\left(e^{-\frac{\pi^2}{12a}}\right), \\ &= \frac{3\sqrt{3}r^2}{4\pi t} - \frac{1}{2}\frac{3\sqrt{3}r}{2\sqrt{\pi t}} + \frac{1}{3} + \mathcal{O}\left(e^{-\frac{\pi^2}{12a}}\right), \\ &= \frac{3\sqrt{3}r^2}{4\pi t} - \frac{6\sqrt{3}r}{8\sqrt{\pi t}} + \frac{1}{3} + \mathcal{O}\left(e^{-\frac{\pi^2}{12a}}\right). \end{aligned} \tag{2.73}$$

And for an equilateral triangle we have that $A = 3\sqrt{3}r^2$, $P = 6\sqrt{3}r$ and $\frac{1}{24}\sum_i \left(\frac{\pi}{\alpha_i} - \frac{\alpha_i}{\pi}\right) = \frac{1}{3}$, again verifying Theorem 2.1.1.

Corollary 2.2.6. *There is no bounded domain in $\mathbb{R}^2$ whose spectrum has the form*

$$\lambda_{m,n} = c(m^2 - mn + n^2). \tag{2.74}$$

Proof. The heat trace of such a domain would be $\bar{h}(t)$, whose asymptotics can be extracted in the same way we did for $h(t)$. Performing this calculation shows that this shape would have twice the area but the same perimeter as an equilateral triangle with inscribed circle radius $r = \sqrt{\frac{27c}{4\pi^2}}$. Since an equilateral triangle has $\frac{A_\Delta}{P_\Delta^2} = \frac{\sqrt{3}}{36}$, this hypothetical shape would have $\frac{2A_\Delta}{P_\Delta^2} = \frac{2\sqrt{3}}{36} > \frac{1}{4\pi}$ and would thus violate the isoperimetric inequality. □

2.3 Hearing the Shape of a Triangle

2.3.1 Outline

In this section we present an elaborated version of the proof given by Grieser and Maronna in [5] that a triangle T is identifiable among all triangles by the eigenvalues of the Laplace operator on T. In other words, when a drum is known to be triangular, the spectrum of the Laplace operator fully determines the angles and size of the drum.

This was not a new result, Durso [3] had proven this already in 1988. The novelty of Grieser and Maronnas proof lies in the fact that while Durso used the wave trace, a complicated object that was not available in the time of Kac, Grieser and Maronna built their proof solely around the heat trace, which was already known by Kac. Central in this proof will be the short time asymptotics from Section 2.1.

For a triangle we have that $\sum_i \alpha_i = \pi$ which means that Theorem 2.1.1 states that

$$h(t) = \frac{A}{4\pi}t^{-1} + -\frac{P}{8\sqrt{\pi}}t^{-\frac{1}{2}} + \frac{1}{24}\left(\sum_{i=1}^{3}\frac{\pi}{\alpha_i} - 1\right) + O\left(e^{-\frac{c}{t}}\right). \tag{2.75}$$

This means that the eigenvalues of the Laplace operator determine the area A, the perimeter P and the quantity $R = \sum_{i=1}^{3}\frac{1}{\alpha_i}$ of a triangle, because they are determined by the heat trace, which in turn is determined by the eigenvalues. What remains to be shown is that these three quantities A, P and R fully determine a triangle. This is what was proven in [5] and leads to the formulation of Theorem 2.3.1.

Theorem 2.3.1. *A triangle is fully determined by the area A, perimeter P and $R = \sum_{i=1}^{3}\frac{1}{\alpha_i}$.*

To show this, we will proof Proposition 2.3.2.

Proposition 2.3.2. *A triple of positive real numbers (α, β, γ) satisfying $\alpha + \beta + \gamma = \pi$ is determined, up to ordering, by the values of $f(\alpha, \beta, \gamma) = \cot\frac{\alpha}{2} + \cot\frac{\beta}{2} + \cot\frac{\gamma}{2}$ and $g(\alpha, \beta, \gamma) = \frac{1}{\alpha} + \frac{1}{\beta} + \frac{1}{\gamma}$.*

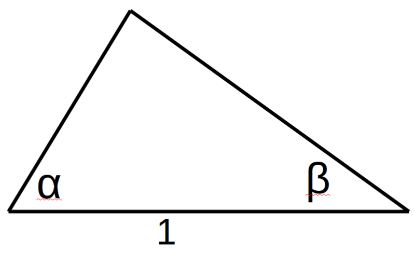

Figure 2.3: The first step in reconstructing a triangle given the interior angles α, β and γ and the perimeter P. This triangle has the correct interior angles but has to be scaled to the correct value of P.

This will be accomplished by examining the behaviour of these functions on $D = \{(\alpha,\beta,\gamma)|\alpha+\beta+\gamma=\pi$ and $\alpha,\beta,\gamma>0\} \subset \mathbb{R}^3_{>0}$ which can be thought of as the space of all triangles up to scaling.

We can then use the identity for triangles

$$\cot\frac{\alpha}{2}+\cot\frac{\beta}{2}+\cot\frac{\gamma}{2}=\frac{P^2}{4A} \tag{2.76}$$

to conclude that A, P and R completely determine the interior angles of a triangle. Now that we know the interior angles, we can construct the triangle in Figure 2.3 which will have some perimeter P_0. The triangle corresponding to A, P and R is then given by the one in Figure 2.3 scaled by a factor of P/P_0.

2.3.2 Proof of Proposition 2.3.2

Before proving Proposition 2.3.2 we will need three somewhat technical lemma's.

Lemma 2.3.3. *The function* $G(x)=\frac{1}{sin^2 x}-\frac{1}{x^2}$ *is strictly increasing and strictly convex on the interval* $(0,\pi)$.

Proof. We start by computing the first two derivatives of G.

$$\begin{aligned} G'(x) &= -\frac{2\cos x}{\sin^3 x}+\frac{2}{x^3}, & (2.77)\\ G''(x) &= \frac{6\cos^2 x}{\sin^4 x}+\frac{2}{\sin^2 x}-\frac{6}{x^4} \\ &= \frac{6}{\sin^4 x}-\frac{4}{\sin^2 x}-\frac{6}{x^4}. & (2.78)\end{aligned}$$

We will now show that $G'(x)$ is positive for all $x\in(0,\pi)$. In view of (2.77) we need to prove the inequality $\frac{2}{x^3}>\frac{2\cos x}{\sin^3 x}$ or equivalently, since $\sin x>0$ for $x\in(0,\pi)$, $\frac{\sin^3 x}{x^3}>\cos x$. To show this, we proceed in steps.

Step I: We will show that

$$\sin x > x-\frac{1}{6}x^3. \tag{2.79}$$

Define $f(x)=x-\frac{1}{6}x^3-\sin x$, we will show that $f(x)<0$ for $x>0$.

$$\begin{aligned} f'(x) &= 1-\tfrac{1}{2}x^2-\cos x, & f'(0)&=0,\\ f''(x) &= -x+\sin x, & f''(0)&=0,\\ f'''(x) &= -1+\cos x, & f'''(0)&=0.\end{aligned}$$

It is clear that $f'''(x) \leq 0$ and equal to zero only if $x = 0 + 2\pi k, k \in \mathbb{Z}$. Then by the fundamental theorem of calculus we have that $f''(x) = f''(0) + \int_0^x f'''(t)dt < 0$ for any $x > 0$. Then we also have $f'(x) = f'(0) + \int_0^x f''(t)dt < 0$ for any $x > 0$ and thus $f(x) = f(0) + \int_0^x f'(t)dt < 0$ for any $x > 0$. This proves the inequality $\sin x > x - \frac{1}{6}x^3$.

Step II: On the interval of interest, $(0, \pi)$, we have that $\sin x > 0$ and $x > 0$ so we also get

$$\frac{\sin^3 x}{x^3} > \frac{\left(x - \frac{1}{6}x^3\right)^3}{x^3} = 1 - \frac{1}{2}x^2 + \frac{1}{12}x^4 - \frac{1}{216}x^6. \tag{2.80}$$

We claim that $\cos x$ is smaller than the right hand side of (2.80). In order to prove this, define $g(x) = 1 - \frac{1}{2}x^2 + \frac{1}{12}x^4 - \frac{1}{216}x^6 - \cos x$, we will show that this function is positive on $(0, \pi)$.

Using the Taylor expansion of $\cos x$ around $x = 0$ we get

$$g(x) = 1 - \frac{1}{2}x^2 + \frac{1}{12}x^4 - \frac{1}{216}x^6 - (1 - \frac{1}{2}x^2 + \frac{1}{4!}x^4 - \frac{1}{6!}x^6 + ...) \tag{2.81}$$

or when simplified

$$\begin{aligned} g(x) = &\left[\frac{1}{24}x^4 - \frac{7}{2160}x^6 - \frac{1}{8!}x^8\right] + \left[\frac{1}{10!}x^{10} - \frac{1}{12!}x^{12}\right] + ... \\ &+ \left[\frac{1}{(2n)!}x^{2n} - \frac{1}{(2n+2)!}x^{2n+2}\right] + ... \end{aligned} \tag{2.82}$$

We will show that all bracketed terms are positive on $(0, \pi)$ separately and that thus their sum $g(x)$ is positive there as well.

The first term is $\frac{1}{24}x^4 - \frac{7}{2160}x^6 - \frac{1}{8!}x^8$. Because $x > 0$ this is greater then 0 if $\frac{1}{24} > \frac{7}{2160}x^2 + \frac{1}{8!}x^4$ holds on $(0, \pi)$. Since the inequality holds for $x = \pi$ and the right hand side of this inequality is clearly an increasing function for positive x, this inequality holds on $(0, \pi)$.

The second term, and all subsequent terms, are of the form $\frac{1}{(2n)!}x^{2n} - \frac{1}{(2n+2)!}x^{2n+2}$ where $n \geq 5$. It is clear that this is positive iff $(2n+2)(2n+1) > x^2$. Since both functions are increasing for $n \geq 5$ and $x > 0$ this inequality will hold in all applicable cases if it holds for $x = \pi$ and $n = 5$, which it clearly does. Therefore $g(x)$ can be written as a sum of positive terms and must consequently be positive.

It now follows that

$$\frac{\sin^3 x}{x^3} > 1 - \frac{1}{2}x^2 + \frac{1}{12}x^4 - \frac{1}{216}x^6 > \cos x \tag{2.83}$$

and thus we conclude that $G'(x) > 0$ for $x \in (0, \pi)$.

Next, we show strict convexity of G on $(0, \pi)$. In other words, we need to show that

$$\frac{6}{\sin^4 x} - \frac{4}{\sin^2 x} - \frac{6}{x^4} > 0 \tag{2.84}$$

This can be rewritten using the positivity of x and $\sin x$ on $(0, \pi)$ as

$$3x^4 > 2x^4 \sin^2 x + 3 \sin^4 x \tag{2.85}$$

Again, we use an estimate for the sine by a polynomial expression;

$$\sin x < x - \frac{1}{3!}x^3 + \frac{1}{5!}x^5. \tag{2.86}$$

This can be proven in a way perfectly analogous to the proof of the inequality in (2.79). (2.86) also provides us with the following two estimates:

$$\sin^2 x < x^2 - \frac{1}{3}x^4 + \frac{2}{45}x^6 - \frac{1}{360}x^8 + \frac{1}{14400}x^{10} \tag{2.87}$$

$$\begin{aligned} \sin^4 x \quad < \quad & x^4 - \frac{2}{3}x^6 + \frac{1}{5}x^8 - \frac{19}{540}x^{10} + \frac{257}{64800}x^{12} - \frac{19}{64800}x^{14} \\ & + \frac{1}{72000}x^{16} - \frac{1}{2592000}x^{18} + \frac{1}{207360000}x^{20} \end{aligned} \tag{2.88}$$

From these estimates it follows that the inequality

$$\begin{aligned} & \left[-\frac{1}{15} - \frac{1}{60}x^2 + \frac{137}{21600}x^4 - \frac{1}{1800}x^6\right] + \left[-\frac{1}{5400}x^6 + \frac{1}{72000}x^8\right] + \\ & \qquad \left[-\frac{1}{2592000}x^{10} + \frac{1}{207360000}x^{12}\right] < 0 \end{aligned} \tag{2.89}$$

implies the inequality in (2.85). We will again consider all terms in brackets separately and show that they are negative, thereby proving the inequality (2.85).

The first term is $p(x) := -\frac{1}{15} - \frac{1}{60}x^2 + \frac{137}{21600}x^4 - \frac{1}{1800}x^6$. This polynomial p tends to $-\infty$ if x tends to ∞. Thus, if all extrema of p are negative, p is negative for $x \in (0, \pi)$. The derivative is $p'(x) = -\frac{1}{30}x + \frac{137}{5400}x^3 - \frac{1}{300}x^5$ of which the zeroes are easily found, namely $x = \pm\frac{1}{6}\sqrt{137 - \sqrt{5809}}$, $x = \pm\frac{1}{6}\sqrt{137 + \sqrt{5809}}$ and $x = 0$. These yield as values for the extrema of p $\frac{\pm 5809^{3/2} - 2891287}{41990400}$ and $-\frac{1}{15}$ respectively, which are all negative. Thus we can conclude that this first term is negative [3].

The second term is $-\frac{1}{5400}x^6 + \frac{1}{72000}x^8$, since x is positive we get that this is negative if $\frac{72000}{5400} > x^2$ for all $x \in (0, \pi)$, which holds already for $x = \pi$ so surely for $x \in (0, \pi)$. The third term follows similarly.

We can now conclude that the inequality in (2.89) does indeed hold and thus we can conclude that $G''(x) > 0$ for all $x \in (0, \pi)$ and thus that G is strictly convex [4]. □

Lemma 2.3.4. *A smooth function $f : (a, b) \to \mathbb{R}$ that is strictly*

a) monotonous
b) convex, or
c) concave

[3] An alternative proof of this uses the Cardano formula. Interpreting p as a third degree polynomial in x^2 we can use the Cardano formula to find the real zero of p as polynomial in x^2. This turns out to be approximately -2, therefore p is zero only when $x^2 = -2$. Form this we can conclude that p has no real zeroes and since p is negative for $x = 0$ p must be negative everywhere.

[4] An alternative proof of this can be found in [5] using partial fractions.

can not have three distinct zeroes.

Proof. **a)** Suppose we have two separate zeroes $x_1 < x_2$, then $f(x_1) = f(x_2)$ with $x_1 < x_2$ contradicts strict monotony.

b) Suppose f is strictly convex, so $f''(x) > 0$ for all $x \in (a, b)$. If $f''(x) > 0$ it follows that $f'(x)$ is strictly increasing. Suppose f has three separate zeroes $x_1 < x_2 < x_3$. Then according to Rolle's theorem, there exist $c_1 \in (x_1, x_2)$ and $c_2 \in (x_2, x_3)$ such that $f'(c_1) = 0$ and $f'(c_2) = 0$. Since we also have $c_1 < x_2 < c_2$ this contradicts the fact that f' is strictly increasing. Therefore we can not have three separate zeroes.

c) Suppose f is strictly concave, then $-f$ is strictly convex by definition and thus $-f$ cannot have three separate zeroes according to b). Since f and $-f$ have the same zeroes it follows that f also cannot have three separate zeroes. □

Before we come to our third lemma we will introduce some terminology. Recall the definition of $D = \{(\alpha, \beta, \gamma) | \alpha + \beta + \gamma = \pi \text{ and } \alpha, \beta, \gamma > 0\}$, we can think of points in D as defining the angles of a triangle. With this in mind we can see that for every triangle there is a corresponding point in D, given by the triple of the interior angles of the triangle. Most triangles have multiple corresponding points in D, each point corresponding to a different ordering of the interior angles. We define isosceles points of D as those points corresponding to an isosceles triangle, or those points where at least two of the coordinates are equal.

Lemma 2.3.5. *We define the functions* $f(\alpha, \beta, \gamma) = \cot\frac{\alpha}{2} + \cot\frac{\beta}{2} + \cot\frac{\gamma}{2}$, $g(\alpha, \beta, \gamma) = \frac{1}{\alpha} + \frac{1}{\beta} + \frac{1}{\gamma}$ *and* $h(\alpha, \beta, \gamma) = \alpha + \beta + \gamma$ *as functions from* $\mathbb{R}^3_{>0} \to \mathbb{R}$.

a) g *is strictly convex on* $\mathbb{R}^3_{>0}$.

b) ∇f, ∇g *and* ∇h *are linearly independent at all nonisosceles points of D.*

Proof. **a)** A function $\mathbb{R}^3_{>0} \to \mathbb{R}$ is strictly convex if the corresponding Hessian is positive definite. The Hessian matrix for g is

$$Hess(g)(\alpha, \beta, \gamma) = \begin{pmatrix} \frac{2}{\alpha^3} & 0 & 0 \\ 0 & \frac{2}{\beta^3} & 0 \\ 0 & 0 & \frac{2}{\gamma^3} \end{pmatrix} \tag{2.90}$$

Since the eigenvalues of $Hess(g)$ are positive, we conclude that g is strictly convex on $\mathbb{R}^3_{>0}$.

b) The gradients of f, g and h are

$$\nabla f = -\frac{1}{2}\begin{pmatrix} \frac{1}{\sin^2\frac{\alpha}{2}} \\ \frac{1}{\sin^2\frac{\beta}{2}} \\ \frac{1}{\sin^2\frac{\gamma}{2}} \end{pmatrix}, \nabla g = -\begin{pmatrix} \frac{1}{\alpha^2} \\ \frac{1}{\beta^2} \\ \frac{1}{\gamma^2} \end{pmatrix}, \nabla h = \begin{pmatrix} 1 \\ 1 \\ 1 \end{pmatrix} \tag{2.91}$$

Suppose ∇f, ∇g and ∇h are linearly dependent at a nonisosceles point $(\alpha, \beta, \gamma) \in D$. So there are R, S, T not all zero with

$$0 = -\frac{R}{2}\begin{pmatrix} \frac{1}{\sin^2\frac{\alpha}{2}} \\ \frac{1}{\sin^2\frac{\beta}{2}} \\ \frac{1}{\sin^2\frac{\gamma}{2}} \end{pmatrix} - S\begin{pmatrix} \frac{1}{\alpha^2} \\ \frac{1}{\beta^2} \\ \frac{1}{\gamma^2} \end{pmatrix} + T\begin{pmatrix} 1 \\ 1 \\ 1 \end{pmatrix} \tag{2.92}$$

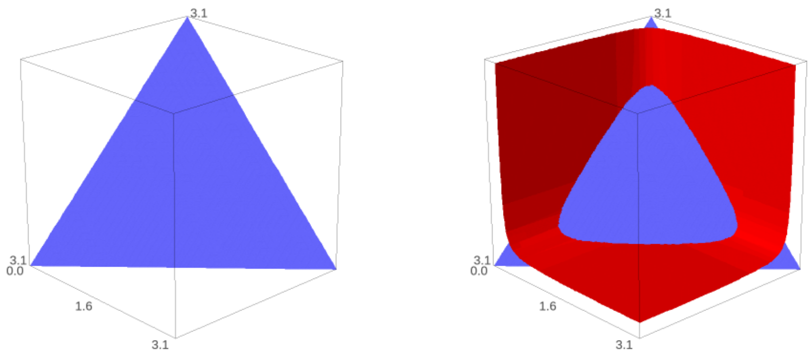

Figure 2.4: On the left an image of D as subset in $\mathbb{R}^3$, on the right D is shown together with a levelset of R in red, the intersection forms the curve in $\mathbb{R}^3$ that the angles (α, β, γ) must be on in order to satisfy a certain value of R.

Clearly, R and S cannot both be zero. This means that the function $F(x) = -\frac{R}{2}\frac{1}{\sin^2\frac{x}{2}} - S\frac{1}{x^2} + T$ has three seperate zeroes, namely $\alpha, \beta, \gamma \in (0, \pi)$. First, if $R \neq 0$, we rewrite F slightly to $F(x) = -\frac{R}{2}\left(\frac{1}{\sin^2\frac{x}{2}} + \frac{S}{2R}\frac{1}{\left(\frac{x}{2}\right)^2}\right) + T$. Then we define $G_C(x) = G(x) + \frac{1-C}{x^2} = \frac{1}{\sin^2 x} - \frac{C}{x^2}$ with $G(x)$ as in Lemma 2.3.3. The function $g_C(x) = \frac{1-C}{x^2}$ has first and second derivatives $g_C'(x) = \frac{-2+2C}{x^3}$ and $g_C''(x) = \frac{6-6C}{x^4}$. From this we can see that for $x \in (0, \pi)$ and $C \geq 1$ that $g_C'(x) \geq 0$ and if $C \leq 1$ that $g_C''(x) \geq 0$. Combining this with Lemma 2.3.3 we find that $G_C(x)$ is strictly increasing for $C \geq 1$ and strictly convex for $C \leq 1$. We then write $F(x) = -\frac{R}{2}G_{-\frac{S}{2R}}(\frac{x}{2}) + T$ from which we can conclude that F is strictly monotonous ($-\frac{S}{2R} \geq 1$), convex ($-\frac{S}{2R} \leq 1$, $\frac{R}{2} < 0$) or concave ($-\frac{S}{2R} \leq 1$, $\frac{R}{2} > 0$).

If $R = 0$ it is also clear that F is strictly monotonous for $x \in (0, \pi)$. It now follows from Lemma 2.3.4 that F cannot have 3 seperate zeroes, and therefore we must conclude that ∇f, ∇g and ∇h are not linearly dependent. □

We now have all the necessary ingredients to prove Proposition 2.3.2.

Proof of Proposition 2.3.2. Figure 2.4 is an illustration of $D \subset \mathbb{R}^3$. If we consider only non-isosceles points D consists of six disjoint connected subsets which we will call chambers. Each triangle is represented six times in the whole of D, once in every chamber, because every chamber corresponds to a different order of naming the angles. We will first show that the sublevel sets of g are convex and then that f is monotone along a level curve of g within a chamber.

Because g is strictly convex by Lemma 2.3.5a) the set $G_{\leq s} = \{p \in \mathbb{R}^3_{>0} | g(p) \leq s\}$ is strictly convex and has boundary $G_s = \{p \in \mathbb{R}^3_{>0} | g(p) = s\}$. Because the value of g is invariant under coordinate permutations the sublevel sets must also be invariant under coordinate permutations. These two properties, convex sublevel sets and invariance, must then also hold for $G_{\leq s} \cap \{(\alpha, \beta, \gamma) | \alpha + \beta + \gamma = \pi\}$.

As one of the angles of a point $p \in \mathbb{R}^3_{>0}$ tends to zero, $g(p)$ tends to infinity. From the arithmetic-harmonic mean inequality

$$3\left(\frac{1}{\alpha} + \frac{1}{\beta} + \frac{1}{\gamma}\right)^{-1} \leq \frac{\alpha + \beta + \gamma}{3} \tag{2.93}$$

we can see that under the constraint $\alpha + \beta + \gamma = \pi$ this becomes

$$\frac{1}{\alpha} + \frac{1}{\beta} + \frac{1}{\gamma} \geq \frac{9}{\pi} \tag{2.94}$$

with equality only if $\alpha = \beta = \gamma = \frac{\pi}{3}$.

From all this it follows that for $s < \frac{9}{\pi}$ the intersection $G_s \cap D$ is empty, for $s = \frac{9}{\pi}$ we have $G_s \cap D = \{e\} = \{(\frac{\pi}{3}, \frac{\pi}{3}, \frac{\pi}{3})\}$ and for any $s > \frac{9}{\pi}$ we finally have that $G_s \cap D$ is a closed curve encircling e. This means that knowing the value of g limits the possible triangles as represented in D to a curve. This means that if the value of g is known for a certain triangle, the points that may correspond to this triangle are limited to a curve in D given by $G_s \cap D$. If we can show that f is strictly monotone along the part of this curve within a chamber, there will only be a single point per chamber that satisfies both the values f and g.

Suppose f is not strictly monotone along a section of the curve $G_s \cap D$ that is within a chamber. We will call the endpoints of this curve p and q, corresponding to isosceles triangles. Then there is a point on the curve, different from p and q, where f is stationary. But according to the Lagrange multiplier theorem this implies that ∇f is a linear combination of ∇g and ∇h, contradicting Lemma 2.3.5b). Therefore f has to be strictly monotone along the curve $G_s \cap D$ within a chamber.

This means that there is at most one point per chamber satisfying certain values for f and g, all corresponding to the same triple, just with different orderings. Therefore f and g determine the triple (α, β, γ) up to ordering, proving Proposition 2.3.2. □

Chapter 3

Wave trace

Analogous to the heat trace for the heat equation on some domain Ω we can define the wave trace, corresponding to the wave equation

$$\begin{cases} (\partial_t^2 - \Delta)u = 0 \\ u(0,x) = f(x) & x \in \Omega \\ \partial_t u(t,x)|_{t=0} = 0 & x \in \Omega \\ u(t,x) = 0 & x \in \partial\Omega \end{cases} \tag{3.1}$$

for $u : [0,\infty) \times \Omega \to \mathbb{R}$. We can again construct a kernel, called the wave kernel, as

$$W(t,x,y) = \sum_{k=1}^{\infty} e^{it\sqrt{-\lambda_k}} u_k(x) u_k(y) \tag{3.2}$$

where u_k is the eigenfunction associated to the eigenvalue λ_k.

The wave trace is then

$$w(t) = \mathrm{Tr}\left(e^{it\sqrt{-\Delta}}\right) \tag{3.3}$$

$$= \sum_{k=1}^{\infty} e^{it\sqrt{-\lambda_k}} \tag{3.4}$$

$$= \int_{\Omega} W(t,x,x)dx. \tag{3.5}$$

As was the case with the heat trace, the wave trace carries geometric information about the domain, which is mainly computed through the third identity, while the second identity shows that the wave trace is a spectral invariant.

Unlike the heat trace, which was a well defined function for all $t > 0$ the wave trace is not defined as a function, but rather as a distribution on $\mathbb{R}$. The fact that the wave trace is a well defined distribution is not immediately obvious and is therefore the subject of next section. The sections after that will describe the geometric information that can be obtained from the wave trace.

3.1 Existence of Wave Trace

3.1.1 Some Summation Results

Before we can show that the wave trace exists as a distribution on $\mathbb{R}$ we need some summation results on the spectrum. From Weyls law, Theorem 1.0.1, we want to deduce the asymptotic growth of the eigenvalues λ_n themselves, for which we use the following lemma.

Lemma 3.1.1. *The counting function given by*

$$N_-(x) = \#\{n|\lambda_n < x\} \tag{3.6}$$

has the same limit as in Theorem 1.0.1.

Proof. We will proof the equivalent limit

$$\lim_{x\to\infty} \frac{N_-(x) - N_+(x)}{x^{d/2}} = 0. \tag{3.7}$$

From the definitions of N_- and N_+ it follows that

$$N_-(x) - N_+(x) = \begin{cases} m(\lambda_n) & x = \lambda_n \\ 0 & x \notin spec(\Delta_\Omega) \end{cases}, \tag{3.8}$$

where $m(\lambda_n)$ is the multiplicity of the eigenvalue λ_n. Since the eigenvalue sequence converges to infinity as n tends to infinity we can proof the limit in (3.7) by showing that the sequence $\left\{\frac{m(\lambda_n)}{\lambda_n^{d/2}}\right\}_{n\in\mathbb{N}}$ converges to zero. To accomplish this we find a new expression for $m(\lambda_n)$ using the eigenvalue counting function N_+. Because the spectrum of $-\Delta_\Omega$ is discrete, for every λ_n we can find an ϵ_n such that

$$m(\lambda_n) = N_+(\lambda_n) - N_+(\lambda_n - \epsilon_n) \tag{3.9}$$

and $\epsilon_{n+1} < \epsilon_n$. We then get

$$\begin{aligned}
\lim_{n\to\infty} \frac{m(\lambda_n)}{\lambda_n^{d/2}} &= \lim_{n\to\infty} \left(\frac{N_+(\lambda_n)}{\lambda_n^{d/2}} - \frac{N_+(\lambda_n - \epsilon_n)}{\lambda_n^{d/2}} \right), \\
&= c_d - \lim_{n\to\infty} \left(\frac{N_+(\lambda_n - \epsilon_n)}{(\lambda_n - \epsilon_n)^{d/2}} \frac{(\lambda_n - \epsilon_n)^{d/2}}{\lambda_n^{d/2}} \right), \\
&= c_d \left(1 - \lim_{n\to\infty} \frac{(\lambda_n - \epsilon_n)^{d/2}}{\lambda_n^{d/2}} \right), \\
&= c_d(1-1), \\
&= 0.
\end{aligned}$$

□

We are now ready to compute the asymptotic behaviour of the eigenvalues themselves.

Theorem 3.1.2. *For the eigenvalues λ_n we have the asymptotic behaviour*

$$\lambda_n \sim n^{\frac{2}{d}}. \tag{3.10}$$

Proof. From Theorem 1.0.1 and Lemma 3.1.1, combined with the fact that the eigenvalues of Δ_Ω diverge as n tends to infinity, we know that the sequences $\left\{\frac{N_+(\lambda_n)}{\lambda_n^{d/2}}\right\}_{n\in\mathbb{N}}$ and $\left\{\frac{N_-(\lambda_n)}{\lambda_n^{d/2}}\right\}_{n\in\mathbb{N}}$ both converge to c_d as n tends to infinity. Since $N_-(\lambda_n) < n \leq N_+(\lambda_n)$ we get the desired limit through the squeeze test. □

Remark 3.1.2.1. *This theorem seems to follow more directly from Weyls law (Theorem 1.0.1) using the intuitive substitutions $x \to \lambda_n$ and $N(\lambda_n) \to n$. The second substitution however is not correct and Lemma 3.1.1 essentially bounds the amount of incorrectness of this substitution, allowing the proof to be completed along this vein anyway.*

This asymptotic behaviour gives us the required tools to proof the final result of this section.

Theorem 3.1.3. *The sum*

$$\sum_{k=1}^{\infty} \frac{1}{\lambda_k^d} \tag{3.11}$$

converges.

Proof. Since all terms in the sum are positive, it suffices to show that the sum is bounded from above. From Theorem 3.1.2 we know that we can find an $N \in \mathbb{N}$ such that for all $n > N$ we get

$$\left| \frac{n}{\lambda_n^{d/2}} - c_d \right| < c_d. \tag{3.12}$$

From this we also get

$$\begin{aligned} 0 < & \frac{n}{\lambda_n^{d/2}} && < c_d + c_d, \\ 0 < & \frac{1}{\lambda_n^{d/2}} && < \frac{2}{n} c_d, \\ 0 < & \frac{1}{\lambda_n^{d}} && < \frac{4}{n^2} c_d^2. \end{aligned}$$

We can then split up the sum to obtain

$$\begin{aligned} \sum_{k=1}^{\infty} \frac{1}{\lambda_k^d} &= \sum_{k=1}^{N} \frac{1}{\lambda_k^d} + \sum_{k=N+1}^{\infty} \frac{1}{\lambda_k^d}, \\ &< \sum_{k=1}^{N} \frac{1}{\lambda_k^d} + \sum_{k=N+1}^{\infty} \frac{4}{n^2} c_d^2, \\ &\leq \sum_{k=1}^{N} \frac{1}{\lambda_k^d} + \frac{2\pi^2}{3} c_d^2, \\ &< \infty. \end{aligned}$$

□

3.1.2 Existence of Wave Trace

In order to show that the wave trace exists as a distribution on $\mathbb{R}$ we will show that the partial sums form a Cauchy sequence in the topology of pointwise convergence and then use completeness of the distributions in this topology to conclude that the wave trace is in fact a well defined distribution.

Theorem 3.1.4. *The sequence $\{w_N\}$ defined by*

$$w_N(t) = \sum_{k=1}^{N} e^{i\sqrt{\lambda_k} t}$$

is a Cauchy sequence of distributions by $w_N(f) = \langle w_N, f\rangle = \int_{\mathbb{R}} w_N(t)f(t)dt$ in the topology of pointwise convergence, i. e. we have that $\langle w_{n+m} - w_n, \varphi\rangle$ tends to zero for all natural numbers m and test functions φ as n tends to infinity.

Proof. Let φ be a test function on $\mathbb{R}$. Define $M := \max_{x\in\mathbb{R}} |\varphi^{(2d)}(x)|$, $L := |\mathrm{supp}(\varphi^{(2d)})|$, the measure of the support of $\varphi^{(2d)}$, and let $\varepsilon > 0$. Since the sum $\sum_{k=1}^{\infty} \frac{1}{\lambda_k^d}$ converges, we can find $N \in \mathbb{N}$ such that $\sum_{k=N+1}^{\infty} \frac{1}{\lambda_k^d} < \frac{\varepsilon}{M\cdot L}$.

Then for any $m \in \mathbb{N}$ and $n > N$ we have that

$$w_{n+m} - w_n = \sum_{k=n+1}^{n+m} e^{i\sqrt{\lambda_k}t}, \tag{3.13}$$

such that

$$\langle w_{n+m} - w_n, \varphi\rangle = \sum_{k=n+1}^{n+m} \int_{-\infty}^{\infty} e^{i\sqrt{\lambda_k}t}\varphi(t)dt. \tag{3.14}$$

Repeatedly applying partial integration to the integral in (3.14) we get that

$$\begin{aligned} \int_{-\infty}^{\infty} e^{i\sqrt{\lambda_k}t}\varphi(t)dt &= 0 + \frac{i}{\sqrt{\lambda_k}} \int_{-\infty}^{\infty} e^{i\sqrt{\lambda_k}t}\varphi'(t)dt, \\ &= ..., \\ &= \frac{i^m}{\lambda_k^{m/2}} \int_{-\infty}^{\infty} e^{i\sqrt{\lambda_k}t}\varphi^{(m)}(t)dt. \end{aligned} \tag{3.15}$$

Choosing $m = 2d$ in (3.15) and applying the triangle inequality for integrals we get

$$\left|\int_{-\infty}^{\infty} e^{i\sqrt{\lambda_k}t}\varphi(t)dt\right| \leq \frac{1}{|\lambda_k|^d} \int_{-\infty}^{\infty} \left|e^{i\sqrt{\lambda_k}t}\right| |\varphi(t)|\, dt \leq \frac{1}{|\lambda_k|^d} M \cdot L. \tag{3.16}$$

Then

$$\begin{aligned} |\langle w_{n+m} - w_n, \varphi\rangle| &\leq \sum_{k=n+1}^{n+m} \frac{1}{|\lambda_k|^d} M \cdot L, \\ &\leq \sum_{k=N+1}^{\infty} \frac{1}{|\lambda_k|^d} M \cdot L, \\ &< \frac{\varepsilon}{M \cdot L} M \cdot L, \\ &= \varepsilon. \end{aligned}$$

This gives us the desired result that w_n is a Cauchy sequence, since for every $\varepsilon > 0$ and test function φ we can find an N such that for all $n > N$ and $m \in \mathbb{N}$ we have that $|\langle w_{n+m} - w_n, \varphi\rangle| < \varepsilon$.

□

Corollary 3.1.5. *The wave trace is a well defined distribution on $\mathbb{R}$.*

Proof. This follows immediately from the completeness of the space of distributions in the topology of pointwise convergence[14, Thm. 6.17, p. 161] and Theorem 3.1.4. □

3.2 Singularities of the Wave Trace

3.2.1 The Poisson Relation

The connection between the wave trace and the geometry of a domain is encoded in the singularities of the wave trace. The main result here is the so called Poisson relation, this relation was first proven by Chazarain[2] and Duistermaat and Guillemin [9] for smooth, compact manifolds without boundary. Later Guillemin and Melrose [6] proved the Poisson relation for smooth compact manifolds with boundary, Wunsch[18] proved it for compact Riemannian manifolds with conic singularities and Durso[3] proved it for polygons in $\mathbb{R}^2$.

The Poisson relation links the singular support of the wave trace to lengths of periodic billiard ball orbits, so before we can properly state this relation we must know what these periodic orbits are.

A billiard ball orbit on a manifold with a smooth boundary is the path an idealized billiard ball would travel when given certain initial position and velocity. This means it travels along geodesics and reflects of the boundaries of the domain according to the law "angle of incidence equals angle reflection." In the case of a flat polygonal domain the vertices introduce a complication, we need to specify what happens when an orbit hits such a vertex, since angle of incidence and angle of reflection are not well defined at that point.

If the angle of the vertex α is $\frac{2\pi}{n}$ for some natural number n, the vertex is called rational. Near this vertex the polygon looks like a cone with opening angle α, which means we can cover $\mathbb{R}^2$ with n of these cones. An incoming orbit is then continued as if it was an orbit in $\mathbb{R}^2$, so straight through, and reflected about the legs of the cones back into the original cone.

If the vertex isn't rational the above procedure cannot be used. In fact, a billiard ball orbit hitting a non rational vertex can be continued in any direction, similar to the situation that occurs when a pebble is dropped in a perfectly still, mathematically ideal, pond. Dropping the pebble causes a circular wavefront to expand, when this wavefront encounters a vertex in the ponds edge it creates a new circular wavefront centered at the vertex.

An orbit that hits at least one non rational vertex is called diffractive, whereas an orbit that does not hit any non rational vertices is called reflective. These orbits can be given as a function $g : [0, \infty) \to \Omega$ such that for all $t \in [0, \infty)$ where $g(t)$ is not a vertex there is some interval $(t - \epsilon, t + \epsilon)$ on which g parametrizes a geodesic by arclength. A periodic orbit is then naturally an orbit $g : [0, \infty) \to \Omega$ such that there is a T with $g(t + T) = g(t)$ for all $t \in [0, \infty)$.

Now that we know what we mean by periodic orbits we can formulate what we mean by the length spectrum of a domain. The length spectrum of Ω, denoted $\mathbb{L}$, is the set of lengths of periodic orbits within Ω,

$$\mathbb{L} = \{T | \text{there exists a } T \text{ periodic billiard ball orbit}\}. \tag{3.17}$$

Iterates of a certain orbit are of course allowed, so if T is in the length spectrum, so is kT for every natural number k. With this in mind we define for a T-periodic orbit g the length, which is T and the primitive length, which is the smallest T' for which $g(t + T') = g(t)$ for all t.

We then have the Poisson relation

$$\text{singsupp}\,(w) \subset \mathbb{L}^+ := \{0\} \cup \pm\mathbb{L}. \tag{3.18}$$

The Poisson relation states that if the wave trace is singular for some value of T there is at least one orbit of length T. It is also known that if there is a unique orbit of a certain length T the wave trace has to be singular at T[3], but if there are multiple geodesics of a certain length T their contributions might cancel each other out, therefore existence of a geodesic of length T is not sufficient to show that the wave trace is singular at T.

3.2.2 Orbits in Triangles

The Poisson relation is a very powerful tool, especially if we know what periodic orbits we can expect for a certain shape. Unfortunately, finding the orbits for a specific shape is in general quite difficult. For triangular domains we do however have some results that will proof useful concerning the shortest periodic orbits.

Theorem 3.2.1 (Durso). *In an acute triangle the Fagnano triangle is the shortest orbit with length*

$$l_{Fagnano} = 2h_i \sin(\alpha_i), \tag{3.19}$$

where h_i is the length of the altitude from angle α_i, followed by the orbit along the altitude from the largest angle of length $2h$, where h is the length of this altitude.

Theorem 3.2.2 (Durso). *In an obtuse triangle the shortest orbit is the one that lies along the altitude from the obtuse angle, of length $2h$ where h is the length of this altitude.*

Durso uses this knowledge to proof that triangles, under some additional assumptions, are spectrally determined. She does this by finding the height from the largest angle from the wave trace, which combined with area and perimeter from the heat trace fixes a triangle. To do this it is necessary to distinguish the singularity due to the Fagnano orbit from the singularity due to the altitude orbit, which she accomplishes by computing the type of singularity due to the altitude orbit, which turns out to be different than the singularity due to the Fagnano orbit. This is used to differentiate between acute and obtuse triangles. The computation of the types of singularities due to certain orbits has since then been generalized by Hillairet.

3.2.3 Nature of the Singularities

In [7] Hillairet computes the nature of the singularities of the wave trace caused by certain geodesics. He provides the behaviour of the quantity

$$I(s) = \langle w_g(t), f(t)e^{-ist} \rangle \tag{3.20}$$

as s tends to infinity. The distribution w_g in this equation is the trace of $e^{it\sqrt{\Delta}}$ microlocalized near a periodic orbit g, it is the contribution to the wave trace by the orbit g. Also, f is a test function localized near the length of g. Finally, for some distribution ϕ and test function $f \in C_c^\infty(\mathbb{R})$ we have written $\phi(f) = \langle \phi, f \rangle$, or in case of the wave trace $w(f) = \langle w(t), f(t) \rangle = \int_{\mathbb{R}} w(t) f(t) dt$.

The exact treatment of microlocalization and the proof of the behaviour (given in Theorem 3.2.3) are beyond the scope of this text but can be found in [7]. However, the associated intuition is as follows. When computing the wave trace we need to integrate the wave kernel over the domain Ω, we integrate separately over the geodesic and the remainder of Ω, this yields w_g and $w - w_g$. If g is the only geodesic of this length, the integral over Ω without the microlocal neighbourhood of g then provides a non singular distribution [8].

It should be noted that Hillairets work is done on a so called Euclidian Surface with Conical Singularities associated to a polygon, which is obtained by glueing two copies of the polygon along the corresponding side. Consequently the wave trace in Hillairets work is obtained by summing over both the Dirichlet and Neumann eigenvalues instead of just the Dirichlet eigenvalues, although all results are claimed to generalize to only the Dirichlet spectrum, all results here are taken directly from Hillairets work and thus concern the combined Dirichlet and Neumann spectrum.

A regular diffractive orbit is any orbit with at least one diffraction such that all angles of diffraction $\beta_i \neq \pm\pi \bmod \alpha_i$. A regular family is a family of non-diffractive orbits such that the diffractive orbits at the limits of the family have only one diffraction.

Theorem 3.2.3 (Hillairet [7]). *For $I(s)$ as in (3.20) we have the following behaviour as s tends to infinity*

i) If g is a regular periodic diffractive orbit of period T and primitive length T_0 we have

$$I(s) \sim s^{-\frac{n}{2}} c_g h(T) e^{-isT} T_0. \tag{3.21}$$

Here $c_g = (2\pi)^{\frac{n}{2}} e^{-\frac{in\pi}{4}} \frac{D_g}{\sqrt{P_g}}$, n is the number of diffractions g undergoes, $D_g = \prod d_{\alpha_i}(\beta_i)$ where α_i is the angle of the ith vertex where g diffracts and β_i is the corresponding angle of diffraction, $d_\alpha(\beta) = -\sum_k \frac{1}{\pi^2-(x+k\alpha)^2}$, and P_g is the product of the lenghts of the different geodesic segments of the orbit.

ii) If g is part of a regular family of periodic orbits of length T we have

$$I(s) \sim s^{\frac{1}{2}} \frac{e^{\frac{i\pi}{4}}}{\sqrt{2\pi}} \frac{1}{\sqrt{T}} h(T) e^{-isT} |A_g| \tag{3.22}$$

where A_g is the area covered by the family. This is actually the contribution of the entire family at once, not of one specific orbit in this family.

Using Theorem 3.2.3 we can see that diffractive orbits with a different number of diffractions will never cancel each other out, since their singularities are of different order.

The following lemma specifies how this behaviour can be computed from the wave trace.

Lemma 3.2.4. *If $w(t)$ is the wave trace of a domain Ω and $f(t) \in C_c^\infty$ such that there is a unique regular diffractive orbit or regular family of orbits g with length $T \in \mathbb{L}^+ \cap \text{supp}(f)$. Then $\langle w(t), f(t)e^{-ist}\rangle \sim \langle w_g(t), f(t)e^{-ist}\rangle$ as s tends to infinity.*

Proof. Since g is assumed to be the only orbit with whose length is in the support of f we know that the singularity at T is due completely to $w_g(t)$[7], and thus that $w - w_g$ is smooth on the support of the test function f since w is smooth but for the contributions of periodic orbits[18].

By the vector space property of distributions we get

$$\langle w(t), f(t)e^{-ist}\rangle = \langle (w - w_g)(t), f(t)e^{-ist}\rangle + \langle w_g(t), f(t)e^{-ist}\rangle. \tag{3.23}$$

This means that we must show that

$$\langle (w - w_g)(t), f(t)e^{-ist}\rangle = \int_{\mathbb{R}} (w - w_g)(t)f(t)e^{-ist}dt = \mathcal{F}\left((w - w_g)f\right)\left(\frac{s}{2\pi}\right) \tag{3.24}$$

tends to zero as s tends to infinity, faster than $\langle w_g(t), f(t)e^{-ist}\rangle$. Here $\mathcal{F}(f) : \mathbb{R} \to \mathbb{C}$ is the Fourier transform of f.

Since $f(t) \in C_c^\infty$ and $w - w_g$ is in $C^\infty(\text{supp}\,(f))$ by assumption, the function $(w - w_g)(t)f(t)$ is also C_c^∞, and thus a Schwartz function on $\mathbb{R}$. Then the Fourier transform $\mathcal{F}\left((w - w_g)f\right)$ is also a Schwartz function [15, Cor. 2.2, p181], and thus goes to zero faster than any $\langle w_g(t), f(t)e^{-ist}\rangle$ from Theorem 3.2.3. □

Chapter 4

Quadrilaterals

To proceed we want to investigate the inverse spectral problem on quadrilaterals. Our primary goal will be to find classes of quadrilaterals such that two isospectral quadrilaterals from such a class must be the same.

Before going into these classes we introduce some of the difficulties related to quadrilaterals over triangles. First of all there is an extra angle to determine, adding one degree of freedom to the problem. On top of that a quadrilateral will usually have two scale parameters instead of one, which can already be seen in the case of the rectangle where both height and width are required. This means that the space of quadrilaterals already has two extra degrees of freedom compared to the space of triangles.

Another complication introduced in the quadrilateral case is the ordering of the angles. In the triangular case a reordering of the angles corresponds to a mirroring of the triangle, which means that the triangles with some area A and angles (α, β, γ) and (α, γ, β) are the same up to an isometry of $\mathbb{R}^2$, which means that the triangles are considered the same. For quadrilaterals this is not true, a quadrilateral with angles $(\alpha, \beta, \gamma, \delta)$ and a quadrilateral with angles $(\alpha, \gamma, \beta, \delta)$ will in general be different, one might for example be a parallelogram while the other is an isosceles trapezium. Thus there is also an extra $\mathbb{Z}_2$ freedom introduced by the step from triangles to quadrilaterals.

Before investigating these different classes separately we will define what specifically these different classes are.

Definition 4.0.5 (Trapezia). *A trapezium is a flat, convex quadrilateral with a pair of parallel sides. The parallel sides are necessarily opposite each other, in the sense that they do not share a vertex.*

Definition 4.0.6 (Overlapping trapezia). *An overlapping trapezium is a trapezium where a section of positive length from one of the parallel sides can be projected perpendicularly onto the other parallel side, see also Figure 4.1.*

Definition 4.0.7 (Acute trapezia). *An acute trapezium is an overlapping trapezium where the vertices of one of the parallel sides are both acute and, consequently, the two vertices of the other parallel side are obtuse. The side with the two acute vertices is necessarily longer than the other parallel side and will be referred to as the base, the other parallel side will be referred to as the top, see also Figure 4.2. Alternatively this class can be characterized by the fact that one of the parallel sides can be completely projected onto the other one.*

Definition 4.0.8 (Obtuse trapezia). *An obtuse trapezium is an overlapping trapezium where both parallel sides have an acute vertex and an obtuse vertex, see also Figure 4.4.*

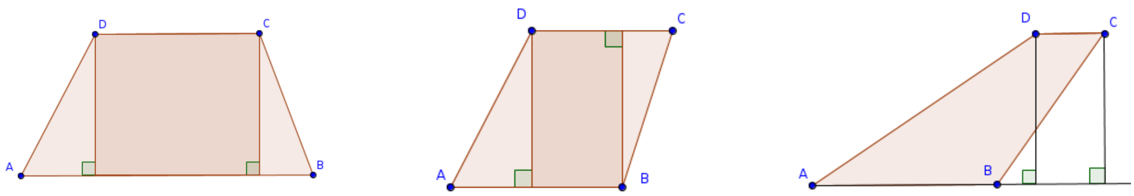

(a) An acute overlapping trapezium

(b) An obtuse overlapping trapezium

(c) Non-overlapping trapezium

Figure 4.1: An overlapping trapezium is a trapezium such that a part of a parallel side can be projected perpendicularly onto the other parallel side.

This can be alternatively characterized by the fact that neither of the parallel sides can be completely projected onto the other one.

4.1 Overlapping Trapezia

Central in our investigation of overlapping trapezia will be a family of orbits, which we will call the height family, that exists precisely because there is overlap. Since part of one parallel side can be projected onto the other perpendicularly we can form a periodic orbit that bounces between the parallel sides, striking each side perpendicularly. The primitive orbits found this way form a regular family in the sense of Theorem 3.2.3, since the bounding orbits travel the altitudes from the obtuse angles of the trapezium, and are thus singly diffractive.

To show that two isospectral acute or obtuse trapezia are identical we will first use the height family to fix the value h and w from Figure 4.2 using the wave trace, then we can fix x and y using the total area A and perimeter P which we get from the heat trace. The difficulties here lie in finding the height family in the wave trace, since it is at this time not clear if this is the shortest family of orbits.

Therefore we will first find some additional restrictions under which we can identify the exact singularity in the wave trace caused by the height family.

Lemma 4.1.1. *Any periodic orbit g that uses the top and base of a trapezium, different from a periodic orbit in the height family, is strictly longer than twice the height.*

Proof. The orbit must travel from some point on the top g_1 to some point on the bottom g_2 and since g is not part of the height family there must be some horizontal displacement $s > 0$, which makes the length of the path from g_1 to g_2 longer than $\sqrt{h^2+s^2}$, so the total path is longer than $2\sqrt{h^2+s^2} > 2h$ since the orbit g must also travel from g_2 back to g_1. □

The above lemma helps us by restricting the possibilities for orbits that are shorter than the height, since we want to find a criterion that lets us locate the singularity caused by the height. We will find that for both acute and obtuse trapezia the only families of orbits that are shorter than the height family must be families of their triangle completions, as described in Definitions 4.1.2 and 4.1.7. The arguments that lead us there differ enough between acute and obtuse trapezia that we will treat them separately.

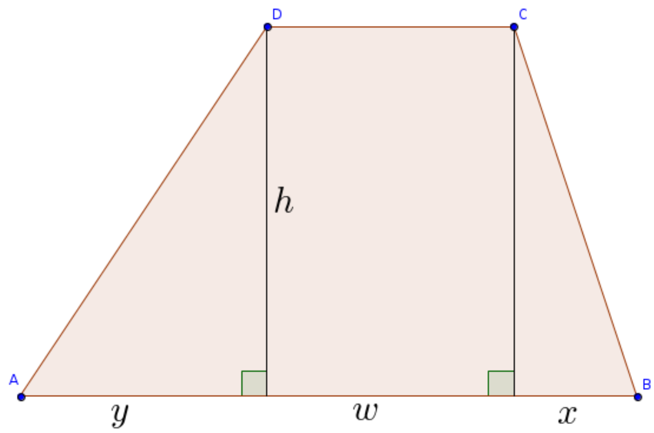

Figure 4.2: An acute trapezium with the four defining lengths we will use throughout this text. We will refer to h as the height and w as the width. This trapezium will be denoted by $\mathcal{T}_{h,w,x,y}$. The requirement in (4.1) states that the longer slanted side must be shorter than the base.

4.1.1 Acute Trapezia

We will denote an acute trapezium by $\mathcal{T}_{h,w,x,y}$ where h, w, x and y refer to the corresponding lengths in Figure 4.2 and we assume, without loss of generality, that $0 \leq x \leq y$, $y > 0$, since swapping x and y corresponds to an isometry and the case where $x = 0$ and $y = 0$ is the rectangle, which can be identified already from the heat trace since $R = \frac{8}{\pi}$ if and only if the trapezium is a rectangle. In fact, in that case height and width can be fully determined from area and perimeter.

Our primary goal here is finding a condition that allows us to locate the singularity due to the height family in the wave trace. To do that we will use Lemma 4.1.1 to get an idea of the shortest possible orbits. In this pursuit we will use the following definition.

Definition 4.1.2. *For an acute trapezium $\mathcal{T}$ we define the associated triangle $\mathcal{T}^+$ defined by the two base vertices of $\mathcal{T}$ and the vertex obtained by intersecting the two non parallel sides, see also Figure 4.3.*

Lemma 4.1.3. *Any periodic orbit other than the height family that is shorter than $2h$ uses exactly the two sides and the base.*

Proof. By Lemma 4.1.1, any orbit other than the height family that uses both the base and the top is strictly longer than $2h$, so any orbit that is shorter than $2h$ must avoid either the base or the top. In an acute trapezium the slanted sides are never parallel, since we demanded $y > 0$, so there are no orbits using only two sides. Furthermore, an orbit that does not use the base has no way to be reflected up again, so can never be periodic. Therefore any orbit that avoids either the top or the base must avoid the top, and must therefore use the sides and the base (possibly multiple times). □

Corollary 4.1.4. *Any periodic orbit of $\mathcal{T}$ shorter than the height family is also an orbit of the associated triangle $\mathcal{T}^+$.*

Lemma 4.1.5. *In an acute trapezium $\mathcal{T}_{h,w,x,y}$ with $0 \leq x \leq y$, $y > 0$ satisfying*

$$\sqrt{h^2 + y^2} < (w + x + y) \tag{4.1}$$

the height family is the shortest family of orbits.

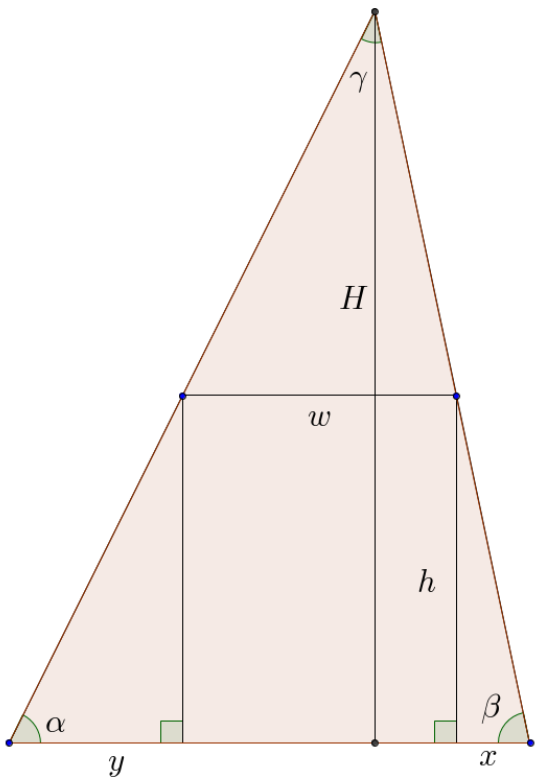

Figure 4.3: The triangle completion associated with the acute trapezium $\mathcal{T}_{h,w,x,y}$, obtained by extending the non parallel sides until they intersect.

Proof. By Corollary 4.1.4 any periodic orbit of $\mathcal{T}$ that is shorter than twice the height must also be an orbit of the associated triangle $\mathcal{T}^+$. We can now use our knowledge about the shortest orbits in a triangle, from Theorems 3.2.1 and 3.2.2, to show that (4.1) guarantees that all families of the triangle $\mathcal{T}^+$ are longer than the height family.

An exercise in trigonometry based on the notation from Figures 4.2 and 4.3 yields the following expressions for the angles of $\mathcal{T}^+$:

$$\sin(\alpha) = \frac{h}{\sqrt{h^2 + y^2}}, \tag{4.2}$$

$$\sin(\beta) = \frac{h}{\sqrt{h^2 + x^2}}, \tag{4.3}$$

$$\sin(\gamma) = \frac{h(x + y)}{\sqrt{h^2 + x^2}\sqrt{h^2 + y^2}}, \tag{4.4}$$

$$\cos(\gamma) = \frac{h^2 - xy}{\sqrt{h^2 + x^2}\sqrt{h^2 + y^2}}. \tag{4.5}$$

If $\mathcal{T}^+$ is obtuse we must have that $\gamma \geq \frac{\pi}{2}$ since α and β are necessarily acute in an acute trapezium, our expression for $\cos(\gamma)$ tells us that this is the case when $h^2 \leq xy$. In an obtuse triangle the shortest periodic orbit is the altitude from the obtuse angle traversed up and down, by Theorem 3.2.2, and thus has length $2H$, which is more than the height family $2h$. Therefore the height family is the shortest family of orbits if $\mathcal{T}^+$

is obtuse. In this case (4.1) is automatically satisfied since

$$\begin{aligned} h^2 &\leq xy, \\ h^2 + y^2 &\leq xy + y^2, \\ h^2 + y^2 &\leq (x+y)^2, \\ \sqrt{h^2 + y^2} &\leq x + y < w + x + y. \end{aligned}$$

If $\mathcal{T}^+$ is acute, so when $h^2 > xy$, then the shortest orbits of the triangle are, in order, the Fagnano triangle and the altitude from the largest angle, by Theorem 3.2.1, which are both isolated orbits. The largest angle of $\mathcal{T}^+$ is either γ or β, since $x \leq y$. If it is γ the height family is shorter than the altitude from γ by the same argument as for the obtuse triangle. If $\beta \leq \gamma < \frac{\pi}{2}$ we have $\sin(\beta) \leq \sin(\gamma)$ and thus $\sqrt{h^2 + y^2} \leq x+y < w+x+y$, so in this case (4.1) is satisfied and not a unnecessary restriction.

If $\beta > \gamma$ the altitude from β is the shortest orbit after the Fagnano triangle, this orbit has length $2(w + x + y)\sin(\alpha)$ or

$$2(w + x + y)\frac{h}{\sqrt{h^2 + y^2}}, \tag{4.6}$$

using our expression for $\sin(\alpha)$ from before. This is longer than the height $2h$ exactly when (4.1) is satisfied, therefore the height family is the shortest family also when $\mathcal{T}^+$ is acute. □

The condition in (4.1) is necessary because we do not know much about the existence of families of orbits in a triangle beyond Theorems 3.2.1 and 3.2.2, i.e. those that are longer than the altitude from the largest angle.

One example of a family of orbits that might be shorter than the height family is due to the Fagnano orbit, when traversed once the Fagnano orbit is isolated, but traversed twice it is actually a part of a family of orbits. This family has length $4H\sin(\gamma)$, in the notation of Figure 4.3, so if γ is small enough this can become smaller than $2h$. If it can be shown that this family is the shortest family in an acute triangle the condition in Lemma 4.1.5 can be relaxed to $\gamma \geq \frac{\pi}{6}$, since then this family can not be shorter than the height family.

Now that we know a condition that allows us to unerringly locate the singularity due to the height family in the wave trace we can move on to a inverse spectral theorem about acute trapezia.

Theorem 4.1.6. *An acute trapezium satisfying* (4.1) *is spectrally determined, in the sense that the defining quantities h, w, x and y can be computed from the spectrum.*

Proof. We start by computing the heat trace, which yields the total area A and perimeter P of our acute trapezium $\mathcal{T}$ by Theorem 2.1.1. Then we will use Lemma 3.2.4 to find the first singularity in the wave trace $w(t)$ corresponding to a family, since only families give singularities of order $\sqrt{s}$, in the notation of Theorem 3.2.3. By lemma 4.1.5 this singularity corresponds to the height family, which means that in the quantity

$$I(s) \sim s^{\frac{1}{2}} \frac{e^{\frac{i\pi}{4}}}{\sqrt{2\pi}} \frac{1}{\sqrt{T}} f(T) e^{-isT} |A_g| \tag{4.7}$$

we have $T = h$ and $|A_g| = hw$. This expression for $I(s)$ allows us to determine T, either by finding how fast $I(s)$ rotates in the complex plane or by varying the test function f.

Therefore we can find h, and through that also w since the value of $|A_g|$ can also be found from $I(s)$ when T is known.

Then we use the formulas

$$A = hw + \frac{1}{2}hx + \frac{1}{2}hy$$
$$P = 2w + x + y + \sqrt{h^2 + x^2} + \sqrt{h^2 + y^2}$$

to solve for x and y. The fact that this yields unique x and y, up to ordering, follows from the fact that the first equality limits a solution (x, y) to a line and the function $f(x, y) = x + y + \sqrt{h^2 + x^2} + \sqrt{h^2 + y^2}$ has Hessian

$$Hess(f)(x, y) = \begin{pmatrix} \frac{h^2}{(h^2+x^2)^{\frac{3}{2}}} & 0 \\ 0 & \frac{h^2}{(h^2+y^2)^{\frac{3}{2}}} \end{pmatrix}, \tag{4.8}$$

which is positive definite, thus the sublevelsets are convex, and the levelsets have at most two intersections with the line defined by the A equality. Since the equations are symmetric in x and y these two solutions must be each others reflection in $y = x$. Existence of a solution is guaranteed by the fact that these A, P, h and w correspond to an actual acute trapezium. As stated earlier, we use the solution with $x \leq y$ without loss of generality.

So we can compute h, w and now x and y from the spectrum, which fixes the acute trapezium. □

4.1.2 Obtuse Trapezia

For obtuse trapezia the method is very similar, although the conditions change slightly. Again we will need to find a condition that is sufficient for us to isolate the singularity due to the height family among all singularities in the wave trace. We will denote an obtuse trapezium by $\mathcal{P}_{h,w,x,y}$ where h, w, x and y refer to Figure 4.4, and we will assume without loss of generality that $0 < x \leq y$, since $\mathcal{P}_{h,w,x,y}$ is $\mathcal{P}_{h,w,y,x}$ rotated by π radians and the cases where $x = 0$ are covered by acute trapezia.

For obtuse trapezia we also define an associated triangle, although it does not exist when $x = y$.

Definition 4.1.7. *For an obtuse trapezium $\mathcal{P}_{h,w,x,y}$ with $x \neq y$ we define the associated triangle $\mathcal{P}^+$ defined by the two base vertices of $\mathcal{P}$ and the vertex obtained by intersecting the two non parallel sides, see also Figure 4.5.*

Lemma 4.1.8. *In an obtuse trapezium $\mathcal{P}_{h,w,x,y}$ satisfying*

$$\sqrt{h^2 + y^2} < w + y, \tag{4.9}$$

the shortest family of orbits is the one consisting of orbits reflecting perpendicularly between the base and top.

Proof. Using Lemma 4.1.1 we know that any orbit shorter than the height can not use both the base and the top, so that leaves three possible sets of sides that the orbit might reflect off of, since there are no possible orbits using only two non parallel sides. These sets are

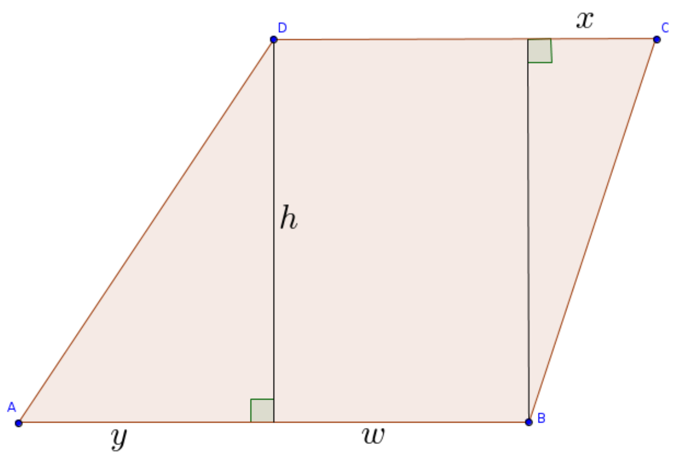

Figure 4.4: An obtuse trapezium with the four defining lengths we will use throughout this text. This trapezium will be denoted by $\mathcal{P}_{h,w,x,y}$. We will refer to h as the height and w as the width. The demand in Lemma 4.1.8, 4.9, states that the slanted side above y must be shorter than the base, the parallel side of length $w + y$.

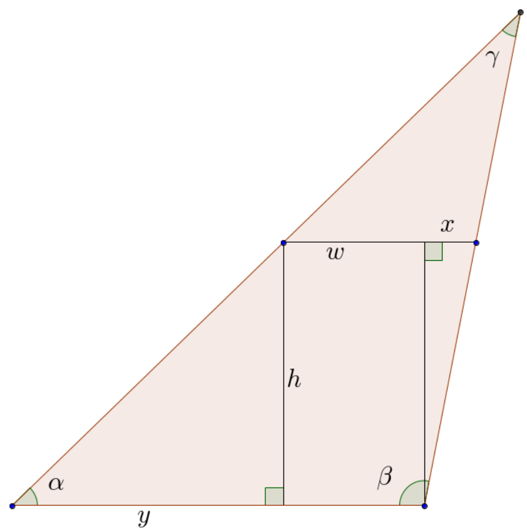

Figure 4.5: The triangle completion associated with the obtuse trapezium $\mathcal{P}_{h,w,x,y}$, obtained by extending the non parallel sides until they intersect.

- the two slanted sides, if they are parallel.
- the two slanted sides and the top.
- the two slanted sides and the base.

The two slanted sides are parallel iff $x = y$, if this is the case there is possibly a family of length $2(w + x)\frac{h}{\sqrt{h^2+x^2}}$. Since we demanded that $w + y > \sqrt{h^2 + y^2}$ and $x = y$, this family is necessarily longer than $2h$.

The only possible periodic orbit using the two slanted sides and the top is the altitude from the obtuse angle between a side and the top, of length $2(w + x)\frac{h}{\sqrt{h^2+x^2}}$, but this is an isolated orbit.

Any orbit using the two sides and the base is also an orbit of the triangle obtained by extending the slanted sides, this triangle is necessarily obtuse, so Theorem 3.2.2 tells us that the shortest orbit of the triangle is the altitude from the obtuse angle, which has length $2(w + y)\frac{h}{\sqrt{h^2+y^2}}$. If $w + y > \sqrt{h^2 + y^2}$, this orbit is necessarily longer than the height family.

Therefore the shortest family is the height family. □

This allows for the proof of the following theorem.

Theorem 4.1.9. *An obtuse trapezium for which* (4.9) *holds is spectrally determined, in the sense that* h, w, x *and* y *can be computed from the spectrum.*

Proof. First we compute the heat trace to find the area A and perimeter P of the obtuse trapezium. Using Lemma 3.2.4 we can find the first singularity in $w(t)$ that corresponds to a family of orbits, since only families can give singularities of order $\sqrt{s}$, in the notation of Theorem 3.2.3. By Lemma 4.1.8 the condition that the trapezium satisfies (4.9) implies that this family is the family of orbits reflecting perpendicularly between the base and the top.

So we can find

$$I(s) \sim s^{\frac{1}{2}} \frac{e^{\frac{i\pi}{4}}}{\sqrt{2\pi}} \frac{1}{\sqrt{T}} f(T) e^{-isT} |A_g| \tag{4.10}$$

for the height family, which means that $T = h$ and $|A_g| = hw$, so h can be computed from the spectrum, either by the speed of rotation of $I(s)$ in the complex plane or by varying the test function f. Once T is known the value of $|A_g|$ is also known, so we can also compute w from the spectrum.

Then we use the formulas

$$A = hw + \frac{1}{2}hx + \frac{1}{2}hy$$
$$P = 2w + x + y + \sqrt{h^2 + x^2} + \sqrt{h^2 + y^2}$$

to solve for x and y. By the same argument as in the corresponding theorem for acute trapezia, Theorem 4.1.6, this yields unique x, y up to ordering, but we chose $x \leq y$ without loss of generality.

Therefore the spectrum fixes h, w, x and y and thus determines the obtuse trapezium. □

4.1.3 Combination of Acute and Obtuse Trapezia

Now we will try to combine these results, the difficulty here will be distinguishing between an acute and obtuse trapezium based on the spectrum. This distinction will have to be made based on the length spectrum, since the acute and obtuse trapezia have some different periodic orbits while all quantities obtained from the heat trace (area, perimeter and R) are the same. It turns out that we can make the distinction, with some severe extra conditions to guarantee existence of certain orbits as well as knowledge of which are the shortest, and these severe conditions still leave some specific cases we have to exclude beforehand.

First we will find the shortest orbits in both acute and obtuse trapezia, using arguments very similar to those in Lemmas 4.1.5 and 4.1.8.

Lemma 4.1.10. *In an acute trapezium satisfying* (4.1) *as well as*

$$h(w+x+y) < \sqrt{h^2+w^2}\sqrt{h^2+y^2} \tag{4.11}$$

and

$$y < \frac{h^2}{w+x}, \tag{4.12}$$

the shortest periodic orbits are the orbits in the height family, Fagnano triangle of the associated triangle and the orbit from the shortest altitude from the base, and the altitude is the longest of the three.

Proof. Any periodic orbit using all four sides must necessarily be longer than $2\sqrt{h^2+w^2}$, since it has a vertical displacement of at least $2h$ and a horizontal displacement of at least $2w$, so the triangle inequality guarantees that the orbit is longer than the mentioned bound.

Therefore the orbits shorter than $2\sqrt{h^2+w^2}$ must be orbits of the associated triangle or use another combination of two or three sides. As mentioned in Lemma 4.1.5 the only option aside from the associated triangle is the height family of length $2h$, which is definitely shorter than $2\sqrt{h^2+w^2}$, and possibly iterates.

The length of the shortest altitude from the base angles is $2(w+x+y)\frac{h}{\sqrt{h^2+y^2}}$, by (4.11) this is shorter than $2\sqrt{h^2+w^2}$. Some trigonometry shows that the height above the base where this altitude meets the opposing slanted side is

$$h' = (w+x+y)\frac{yh}{h^2+y^2}. \tag{4.13}$$

This altitude exists within the trapezium only if this is shorter than h, so we need

$$(w+x+y)y < h^2+y^2 \tag{4.14}$$

which simplifies to the inequality $y < \frac{h^2}{w+x}$ we demanded, therefore this altitude is in fact an orbit of the trapezium.

The Fagnano triangle has length twice an altitude times the sine of the angle the altitude is from, and this works for all altitudes in the triangle. That means that in this case we have a Fagnano triangle orbit of length

$$2(w+x+y)\frac{h^2}{\sqrt{h^2+x^2}\sqrt{h^2+y^2}}, \tag{4.15}$$

and it exists whenever both altitudes from the base angles exist, so when both $y < \frac{h^2}{w+x}$ and $x < \frac{h^2}{w+y}$ are satisfied, this second inequality follows from the first when $x \leq y$. The length of this orbit is also shorter than the shorter altitude, and therefore shorter than $2\sqrt{h^2+w^2}$.

These three are the shortest orbits, since we demanded through (4.1) that the height family is shorter than the short altitude and the shortest two orbits of the associated triangle are the Fagnano triangle and the short altitude. Any other orbit longer than the short altitude. □

Lemma 4.1.11. *In an obtuse trapezium satisfying* (4.9),

$$h(w+y) < \sqrt{h^2+w^2}\sqrt{h^2+y^2} \tag{4.16}$$

and

$$y < \frac{h^2}{w} \tag{4.17}$$

the shortest orbits are the altitudes from the top and base and the height family.

Proof. We use the same reasoning as in Lemma 4.1.10 and Lemma 4.1.8. Any orbit using all four sides is necessarily longer than $2\sqrt{h^2+w^2}$, thus the only orbits that can be shorter are the height family, the shorter altitude and any orbit from the associated triangle, since we showed in Lemma 4.1.8 that these are the only possible orbits not using all four sides.

The height family is of length $2h$ and thus certainly shorter than $2\sqrt{h^2+w^2}$. The shorter altitude has length $2(w+x)\frac{h}{\sqrt{h^2+x^2}}$, and the shortest orbit of the associated triangle is the altitude from the obtuse angle and has length $2(w+y)\frac{h}{\sqrt{h^2+y^2}}$. These altitudes do not always exist as orbits of the trapezium, some trigonometry shows that the longer altitude exists when $y < \frac{h^2}{w}$ and the shorter when $x < \frac{h^2}{w}$, so since $x \leq y$ the demand $y < \frac{h^2}{w}$ suffices to guarantee existence of both.

Then (4.16) ensures that the longer altitude is shorter than $2\sqrt{h^2+w^2}$, which ensures that these three orbits are in fact the shortest of the obtuse trapezium, since these are the shortest orbits using a maximum of three sides and any orbit using all four sides is necessarily longer than $2\sqrt{h^2+w^2}$.

□

Theorem 4.1.12. *A trapezium that is either acute or obtuse is spectrally determined, in the sense that the values of h, w, x and y can be determined and it can be decided whether it is acute or obtuse from the spectrum, provided it satisfies* (4.9), (4.11), (4.12), $0 < x < y$ *and* $\frac{w+x}{\sqrt{h^2+x^2}}$ *and* $\frac{w+y}{\sqrt{h^2+y^2}}$ *are not both natural numbers.*

Proof. Since $x > 0$ we know that (4.9) implies (4.1). Therefore we can use Theorems 4.1.6 and 4.1.9, to find the values of h, w, x and y whether the spectrum corresponds to an acute or an obtuse trapezium, and they will be the same set of values for both. Therefore we only need to distinguish between acute and obtuse based on the spectrum.

Since $x > 0$ we also know that (4.12) implies (4.17) and that (4.11) implies (4.16). Therefore we know that if the spectrum corresponds to an obtuse trapezium the shortest orbits beside the height family are the two altitudes of lengths

$$l_1 = 2(w+x)\frac{h}{\sqrt{h^2+x^2}}, \tag{4.18}$$

$$l_2 = 2(w+y)\frac{h}{\sqrt{h^2+y^2}}. \tag{4.19}$$

While if the spectrum corresonds to an acute trapezium instead, the shortest orbits beside the height family are the Fagnano triangle and the shorter altitude from a base angle, which have lengths

$$L_1 = 2(w+x+y)\frac{h^2}{\sqrt{h^2+x^2}\sqrt{h^2+y^2}}, \tag{4.20}$$

$$L_2 = 2(w+x+y)\frac{h}{\sqrt{h^2+y^2}}. \tag{4.21}$$

We have that $l_1 \leq l_2 < L_1 \leq L_2$ since $w+y < (w+x+y)\frac{h}{\sqrt{h^2+x^2}}$, because the right hand side is increasing in x and then

$$w+y < (w+x+y)\frac{h}{\sqrt{h^2+x^2}}, \tag{4.22}$$

$$(w+y)\frac{h}{\sqrt{h^2+y^2}} < (w+x+y)\frac{h^2}{\sqrt{h^2+x^2}\sqrt{h^2+y^2}}, \tag{4.23}$$

$$l_2 < L_1. \tag{4.24}$$

This means that an acute trapezium can not have singularities at l_1 and l_2, except if iterates of the orbits in the height family cause these singularities. These iterates have length $2nh$ for some $n \in \mathbb{N}$. Since not both $\frac{w+x}{\sqrt{h^2+x^2}}$ and $\frac{w+y}{\sqrt{h^2+y^2}}$ are natural numbers, not both l_1 and l_2 can be $2nh$ for some $n \in \mathbb{N}$.

If $w(t)$ is singular at the l_i that is not $2nh$, the spectrum must correspond to a obtuse trapezium, since an acute trapezium can not have an orbit of this length, while if $w(t)$ is not singular at l_i the spectrum must correspond to an acute trapezium, since an obtuse trapezium must have a singularity at this length.

Therefore we can tell whether the spectrum corresponds to an acute or obtuse trapezium, which concludes this proof. □

Remark 4.1.12.1. *For the sake of clarity we will list all requirements of the above theorem once more*

$$\sqrt{h^2+y^2} < w+y,$$
$$h(w+x+y) < \sqrt{h^2+w^2}\sqrt{h^2+y^2}.$$

Combining these two we need

$$h\sqrt{h^2+y^2} < h(w+y) < h(w+x+y) < \sqrt{h^2+w^2}\sqrt{h^2+y^2}. \tag{4.25}$$

Furthermore we need

$$y < \frac{h^2}{w+x}. \tag{4.26}$$

And finally $\frac{w+x}{\sqrt{h^2+x^2}}$ and $\frac{w+y}{\sqrt{h^2+y^2}}$ are not both natural numbers. Figure 4.6 shows the allowed x and y values for some given h and w.

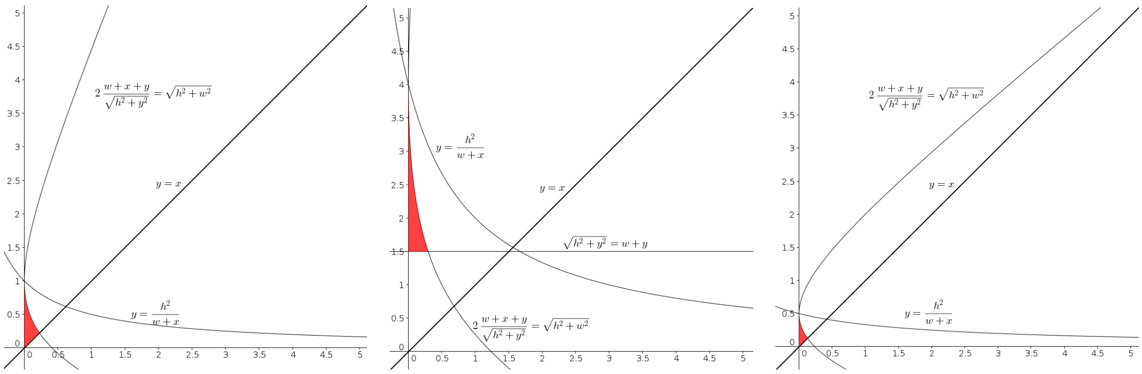

(a) $h = 1$, $w = 1$ (b) $h = 2$, $w = 1$ (c) $h = 1$, $w = 2$

Figure 4.6: Three plots of the inequalities that allow for the application of Theorem 4.1.12 for different values of h and w. A point (x, y) corresponds to values of x and y in the natural way. The lines that bound the regions where (4.9), (4.11) and (4.12) hold are drawn and labelled with the corresponding equality. The shaded area is the region where all inequalities are satisfied and thus represents the allowable trapezia in Theorem 4.1.12. In subfigures a and c (4.9) is satisfied for all $y > 0$, so the inequality is not shown.

So we can determine trapezia in several subclasses spectrally, there are three areas where these subclasses can be extended. Firstly, if we can find a better characterization of orbits in a triangle, or families of orbits in particular, the requirements for Lemmas 4.1.5 and 4.1.8 can be relaxed, which relaxes the conditions for Theorems 4.1.6, 4.1.9 and 4.1.12.

Secondly, a more in depth characterization of orbits in a trapezium could relieve the restrictions added in Theorem 4.1.12 over the restrictions inherited from Theorems 4.1.6 and 4.1.9. If more orbits are characterized, the conditions that currently guarantee existence of the few known orbits that are used to determine whether the spectrum originates from an acute or obtuse trapezium might be relaxed, since more orbits are available to make this distinction.

Finally, in this thesis no arguments have been made for trapezia without overlap. The constructed framework that characterizes the shortest orbits of obtuse overlapping trapezia could be extended to non overlapping trapezia, which are necessarily obtuse. Their length might provide enough information to cover for the missing height family. In order to distinguish overlapping and non overlapping trapezia based on their spectra the lack of a height family might actually be beneficial, but more work on the first point of these three would be required to make this rigorous.

Bibliography

[1] D.L. Webb C. Gordon and S. Wolpert. One cannot hear the shape of a drum. *Bulletin of the American Mathematical Society*, 27(1):134–138, 1992.

[2] J. Chazarain. Formule de Poisson pour les variétés Riemanniennes. *Inventiones mathematicae*, 24:65–82, 1974.

[3] C. Durso. *On the inverse spectral problem for polygonal domains*. PhD thesis, Ph. D. Thesis, MIT, 1988.

[4] H.P.W. Gottlieb. Eigenvalues of the Laplacian for rectilinear regions. *The Journal of the Australian Mathematical Society. Series B. Applied Mathematics*, 29(03):270–281, 1988.

[5] D. Grieser and S. Maronna. Hearing the shape of a triangle. *Notices of the AMS*, 60(11), 2013.

[6] V. Guillemin and R. Melrose. The Poisson summation formula for manifolds with boundary. *Advances in Mathematics*, 32(3):204–232, 1979.

[7] L. Hillairet. Contribution of periodic diffractive geodesics. *Journal of Functional Analysis*, 226(1):48–89, 2005.

[8] L. Hillairet. private communication, 5 2015.

[9] V.W. Guillemin J.J.Duistermaat. The spectrum of positive elliptic operators and periodic bicharacteristics. *Inventiones mathematicae*, 29:39–80, 1975.

[10] M. Kac. Can one hear the shape of a drum? *American Mathematical Monthly*, pages 1–23, 1966.

[11] B.J. McCartin. *Laplacian eigenstructure of the equilateral triangle*. Hikari, Limited, 2011.

[12] J. Milnor. Eigenvalues of the Laplace operator on certain manifolds. *Proceedings of the National Academy of Sciences of the United States of America*, 51(4):542, 1964.

[13] M. Nica. Eigenvalues and Eigenfunctions of the Laplacian. *The Waterloo Mathematics Review*, 1(2):23–34, 2011.

[14] W. Rudin. *Functional analysis. International series in pure and applied mathematics*. McGraw-Hill, Inc., New York, 1991.

[15] E.M. Stein and R. Shakarchi. *Fourier analysis, an introduction*. Princeton University Press, 2003.

[16] E.M. Stein and G.L. Weiss. *Introduction to Fourier analysis on Euclidean spaces*. Princeton university press, 1971.

[17] M. van den Berg and S. Srisatkunarajah. Heat equation for a region in $\mathbb{R}^2$ with a polygonal boundary. *Journal of the London Mathematical Society*, 37(1):119–127, 1988.

[18] J. Wunsch. A Poisson relation for conic manifolds. *arXiv preprint math/0202264*, 2002.